Catalysis Science & Technology

ROYAL SOCIETY OF CHEMISTRY

PAPER

View Article Online
View Journal | View Issue

Check for updates

Cite this: *Catal. Sci. Technol.*, 2020, **10**, 1619

Use of titanocalix[4]arenes in the ring opening polymerization of cyclic esters†

Ziyue Sun,[a] Yanxia Zhao,*[a] Orlando Santoro,[b] Mark R. J. Elsegood,[c] Elizabeth V. Bedwell,[c] Khadisha Zahra,[d] Alex Walton[d] and Carl Redshaw*[ab]

The known dichloride complexes $[TiCl_2L(O)_2(OR)_2]$ (type I: R = Me (**1**), *n*-Pr (**2**) and *n*-pentyl (**3**); $L(OH)_2(OR)_2$ = 1,3-dialkyloxy-*p*-*tert*-butylcalix[4]arene), together with the new complexes $\{[TiL(O)_3(OR)]_2(\mu\text{-}Cl)_2\}$·6MeCN (R = *n*-decyl (**4**·6MeCN)), and $[Ti(NCMe)Cl(L(O)_3(OR))]$·MeCN (type II: R = Me, **5**·MeCN) are reported. Attempts to prepare type II for R = *n*-Pr and *n*-pentyl using $[TiCl_4]$ resulted in the complexes $\{[TiL(O)_3(On\text{-propyl})]_2(\mu\text{-}Cl)(\mu\text{-}OH)\}$ **6**·7MeCN and $\{[TiL(O)_3(On\text{-pentyl})]_2(\mu\text{-}Cl)(\mu\text{-}OH)\}$·7.5MeCN (**7**·7.5MeCN), respectively; use of $[TiCl_4(THF)_2]$ resulted in a co-crystallized THF ring-opened product $[Ti(NCMe)(\mu_3\text{-}O)L(O)_4TiCl(O(CH_2)_4Cl)]_2$–$2[TiCl(NCMe)(L(O)_3(On\text{-}Pr))]$·11MeCN (**8**·11MeCN). The molecular structures of **2**·2MeCN, **4**·6MeCN, and **5**·MeCN together with the hydrolysis products $\{[TiL(O)_3(OR)]_2(\mu\text{-}Cl)(\mu\text{-}OH)\}$ (R = *n*-Pr **6**·7MeCN; *n*-pentyl, **7**·7.5MeCN, **9**·9MeCN); R = *n*-decyl **10**·8.5MeCN) and that of the ring opened product **8**·11MeCN and the co-crystallized species $[Ti_2(OH)Cl(L(O)_3(OR))][L(OH)_2(OR)_2]$ ·$2.85(C_2H_3N)$·$0.43(H_2O)$ (R = *n*-pentyl, **11**·$2.85(C_2H_3N)$·$0.43(H_2O)$) are reported. Type I and II complexes have been screened for their ability to act as catalysts in the ring opening polymerization (ROP) of ε-caprolactone (ε-CL), δ-valerolactone (δ-VL), ω-pentadecalactone (ω-PDL) and *rac*-lactide (*r*-LA), both with and without benzyl alcohol present and either under N_2 or in air. The copolymerization of ε-CL with δ-VL and with *r*-LA has also been investigated. For the ROP of ε-CL, all performed efficiently (>99% conversion) at 130 °C over 24 h both under N_2 and in air, whilst over 1 h, for the type I complexes the trend was **3** > **2** > **1** but all were poor (≤12% conversion). By contrast, **5** over 1 h at 130 °C was highly active (85% conversion). At 80 °C, the activity trend followed the order **5** ≈ **4** > **3** > **2** > **1**. For δ-VL, at 80 °C the activity trend **5** ≈ **4** > **1** > **2** > **3** was observed. ROP of the larger ω-PDL was only possible using **5** at 130 °C over 24 h with moderate activity (48% conversion). For *r*-LA, only low molecular weight products were obtained, whilst for the co-polymerization of ε-CL with δ-VL using **5**, high activity was observed at 80 °C affording a polymer of molecular weight >23 000 Da and with equal incorporation of each monomer. In the case of ε-CL/*r*-LA co-polymerization using **5** either under N_2 or air, the polymerization was more sluggish and only 65% conversion of CL was observed and the resultant co-polymer had 65 : 35 incorporation. Complex **5** could also be supported on silica, however this system was not as active as its homogeneous counterpart. Finally, the activity of these complexes is compared with that of three benchmark species: a di-phenolate Ti compound $\{TiCl_2(2,2'\text{-}CH_3CH[4,6\text{-}(t\text{-}Bu)_2C_6H_2O]_2)\}$ (**12**) and a previously reported NO_2-containing titanocalix[4]arene catalyst, namely cone-5,17-bis-*tert*-butyl-11,23-dinitro-25,27-dipropyloxy-26,28-dioxo-calix[4]arene titanium dichloride (**13**), as well as $[Ti(Oi\text{-}Pr)_4]$; the parent calixarenes were also screened.

Received 20th December 2019,
Accepted 25th January 2020

DOI: 10.1039/c9cy02571e

rsc.li/catalysis

Open Access Article. Published on 27 2020. Downloaded on 10-11-2024 06:39:06.
This article is licensed under a Creative Commons Attribution 3.0 Unported Licence.

Introduction

Metallocalixarenes have attracted a significant amount of interest in the catalysis field, and have found application for a variety of processes.[1] In terms of titanocalixarenes, which date back to the 1980s,[2] Frediani, Sémeril *et al.* employed the 1,3-di-*n*-propyloxycalix[4]arene, $1,3\text{-}L(OH)_2(n\text{-}PrO)_2$, containing complex $[1,3\text{-}L(O)_2(n\text{-}PrO)_2TiCl_2]$, in conjunction with MAO (methylaluminoxane), to afford ultrahigh molecular weight polyethylene.[3] The active species, as determined by ^{1}H NMR

[a] *College of Chemistry and Material Science, Northwest University, 710069 Xi'an, China*
[b] *Plastics Collaboratory, Department of Chemistry and Biochemistry, The University of Hull, Cottingham Rd, Hull, HU6 7RX, UK. E-mail: c.redshaw@hull.ac.uk*
[c] *Chemistry Department, Loughborough University, Loughborough, Leicestershire, LE11 3TU, UK*
[d] *Department of Chemistry and Photon Science Institute, University of Manchester, Oxford Road, Manchester, M13 9PL, UK*

† Electronic supplementary information (ESI) available. CCDC 1954689–1954697 and 1969053. For ESI and crystallographic data in CIF or other electronic format see DOI: 10.1039/c9cy02571e

Open Access Article. Published on 27 2020. Downloaded on 10-11-2024 06:39:06.
This article is licensed under a Creative Commons Attribution 3.0 Unported Licence.

spectroscopy, was determined to be a titanium methyl cation, as observed in earlier work by Proto *et al.*[4] Subsequently, Taoufik, Bonnamour *et al.* extended these studies and investigated the effect of varying the 1,3-dialkyloxy R groups (for R = methyl, ethyl, *n*-propyl and *i*-butyl) on the catalytic activity during ethylene polymerization. In the same study, a couple of 1,2-dialkoxycalix[4]arene derivatives were also prepared, namely the methyloxy and a complex containing a chelating siloxide $SiMe_2$, together with a number of depleted calix[4]arene complexes bearing 1,2- or 1,3-titanium dichloride motifs.[5] Whilst the behavior of the 1,2- and 1,3-systems was different, it was determined that within each series, increasing the number of alkyloxy groups present was detrimental to the catalytic activity. On variation of the R group from methyl to isobutyl in the 1,3-systems, there was no clear structural activity trend. A number of other, less well-defined, titanium calix[*n*]arenes have also been employed for ethylene polymerization.[6] We also note that this type of titanocalix[4]arene has been grafted onto silica and employed in olefin epoxidation by the group of Katz.[7]

With regard to the ring opening polymerization (ROP) of cyclic esters, reports using titanocalix[*n*]arenes are scant. Frediani, Sémeril *et al.* employed the complex {[1,3-*p*-*tert*-butyl-2,4-(NO_2)L$(O)_2$(*n*-PrO)$_2$-1,3]$TiCl_2$}, under solvent-free conditions, for the well-controlled ROP of lactide.[8] The resultant polymer was highly isotactic, whilst the addition of *n*-butanol led to an increase in both the rate of polymerization and transfer with the monomer. The same group also employed complex [1,3-L$(O)_2$(*n*-PrO)$_2$$TiCl_2$] for the ROP of *rac*-lactide (*r*-LA), initiating the catalyst either by use of microwave radiation or heat.[9] Although the rate of polymerization was enhanced by using microwaves, this was to the detriment of control. More recently, McIntosh *et al.* reported preliminary studies on the use of the complex [$Ti_4L^2(O)_8$(O*n*-Pr)$_8$$(THF)_2$] (where $L^2(OH)_8$ = *p*-*tert*-butylcalix[8]-arene) as a catalyst for the ROP of *r*-LA at 130 °C.[10] We have also investigated the use of metallocalix[*n*]arenes for the ROP of cyclic esters such as ε-caprolactone, and have reported how, for a series of tungstocalix[6 and 8]arenes, different sized rings and their associated conformations can drastically affect the catalytic activity.[11] Molybdo- and tungstocalix[4]-arenes were found to be less active.[12] Herein, we have screened several titanocalix[4]arenes, namely [$TiCl_2$L$(O)_2$-$(OR)_2$] (type I: R = Me (**1**), *n*-Pr (**2**) and *n*-pentyl (**3**)), the dimeric compound {[TiL$(O)_3$(OR)]$_2$(μ-$Cl)_2$} (R = *n*-decyl (**4**)), and [Ti(NCMe)Cl(L$(O)_3$(OR))]·MeCN (type II, R = Me, **5**·MeCN, R = *n*-propyl **6** and *n*-pentyl **7**) for the ROP of ε-CL, δ-VL and *r*-LA (the copolymerization of ε-CL and *r*-LA was also investigated) (Chart 1).

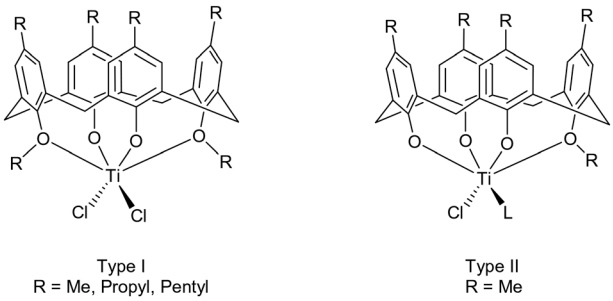

Chart 1 Types I and II titanocalix[4]arenes complexes employed herein for the ROP of ε-CL, δ-VL and *r*-LA.

Results and discussion

Interaction of 1,3-dialkoxycalix[4]arenes, L$(OH)_2(OR)_2$, with [$TiCl_4$] or [$TiCl_4(THF)_2$] is known to readily afford titanocalix[4]arene dichlorides of the type [$TiCl_2$L$(O)_2$-$(OR)_2$].[5,13] We have prepared herein the derivatives where R = Me (**1**), *n*-Pr (**2**) and *n*-Pent (**3**) as reported by Taoufik and Bonnamour, employing acetonitrile as the solvent of crystallization during the workup (Scheme 1).

The structure of the *n*-Pr derivative as the MeCN solvate [$TiCl_2$(L$(O)_2$(O*n*-Pr)$_2$)]·2MeCN (**2**·2MeCN) (CCDC 1954692) is shown in Fig. 1, with selected bond lengths and angles given in the caption. The Ti(IV) center exhibits a slightly distorted octahedral geometry and bears *cis* chlorides. There is a pinched cone calix[4]arene conformation, but with the O(1) side more splayed out than the other at O(3). One MeCN resides inside the calix[4]arene cone with the methyl group most deeply embedded, the other lies *exo*. The molecules of [$TiCl_2$(L$(O)_2$(O*n*-Pr)$_2$)]·2MeCN (**2**·2MeCN) pack in anti-parallel layers with no significant intermolecular interactions (see Fig. S1, ESI†).

In the case of R = *n*-decyl, prolonged standing at 0 °C afforded large red prisms suitable for X-ray crystallography. The molecular structure (CCDC 1954693) is shown in Fig. 2, with selected bond lengths and angles given in the caption. The structure of **4** is a chloro-bridged dimer {[TiL$(O)_3$(OR)]$_2$(μ-$Cl)_2$} (R = *n*-decyl), in which each titanium center is best described as distorted octahedral. The asymmetric unit contains two half molecules both on inversion centers as well as six molecules of crystallization (MeCN). There are weak C–H···O hydrogen bonds between the first CH_2 group of the *n*-decyl chain and a phenolate oxygen on the symmetry related calix[4]arene. The two half molecules differ in two respects. Firstly, the *n*-decyl chains have different conformations at their tails and one is disordered here, while the other is not. Secondly, the number of MeCN molecules in the calixarene cavities is different.

For our subsequent catalytic studies, *vide infra*, we also employed a modification of the Floriani procedure for targeting monochloro titanium calix[4]arenes.[13] In our work, LH_2Me_2 was refluxed with [$TiCl_4(THF)_2$] in toluene (60 h reflux) and then with acetonitrile (24 h) which afforded, on cooling, orange red prisms of [Ti(NCMe)Cl(L$(O)_3$(OR))]·MeCN (**5**·MeCN) in good yield (Scheme 2a).

The structure (CCDC 1954694) is shown in Fig. 3, with selected bond lengths and angles given in the caption. The structure is non-merohedrally twinned *via* a 180° rotation about the direct axis (1 0 0). There are two titanocalix[4]arene

 This journal is © The Royal Society of Chemistry 2020

Open Access Article. Published on 27 2020. Downloaded on 10-11-2024 06:39:06.
This article is licensed under a Creative Commons Attribution 3.0 Unported Licence.

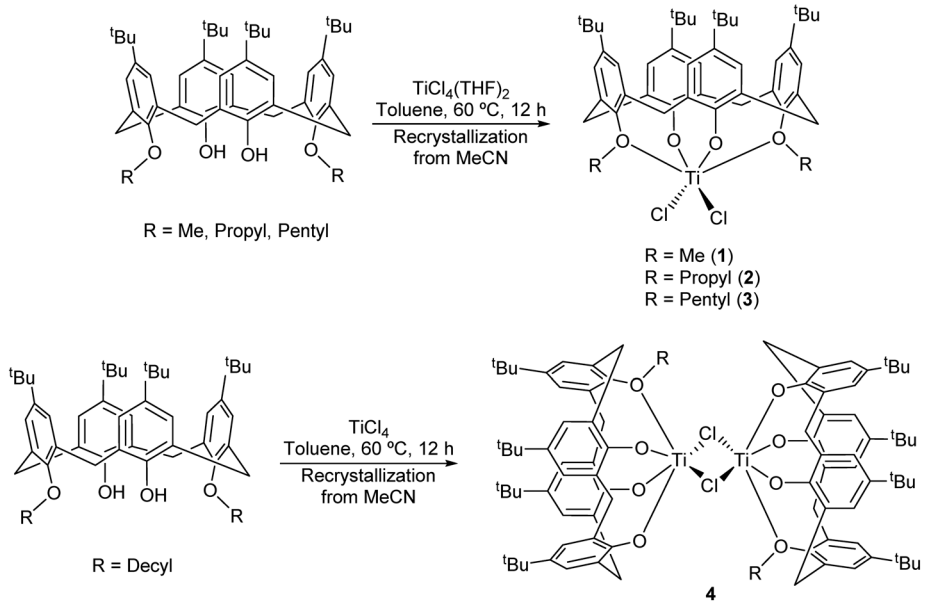

Scheme 1 Synthesis of complexes **1**–**4**.[5]

complexes (related *via* mirror symmetry) and two acetonitrile molecules in the asymmetric cell. The coordination geometry about the distorted octahedral titanium center comprises *cis* chloride and acetonitrile ligands together with a monomethoxycalix[4]arene, the latter adopting a 'down, down, down, out' conformation. The acetonitriles of crystallization reside with their methyl groups inside the calix[4]arene cavities.

We note that a route to monofunctionalised calix[4]arenes *via* removal of an ether functionality using $TiCl_4$ has been reported by Floriani and coworkers.[13] Floriani *et al.* identified CH_3Cl in their reaction and suggested this was the result of capture of the leaving group by the Cl^- nucleophile. We also noted dealkylation when studying the air stability of the type I complex with R = *n*-pentyl.[14] In the case of **5**, this can be viewed as the acetonitrile trapped titanium intermediate en-route to the formation of the monoalkoxycalix[4]arene. Surprisingly, on extension of this methodology to the systems derived from $L(OH)_2(OR)_2$ (R = *n*-propyl or *n*-pentyl), the corresponding monochloride complexes $[Ti(NCMe)Cl(L(O)_3(OR))]\cdot MeCN$ (R = *n*-propyl and *n*-pentyl) were not accessible (Scheme 2b). It was postulated that the de-alkylation of the calix[4]arenes bearing *n*-propyl and *n*-pentyl moieties does not proceed as per their methoxy analogue due to the nature

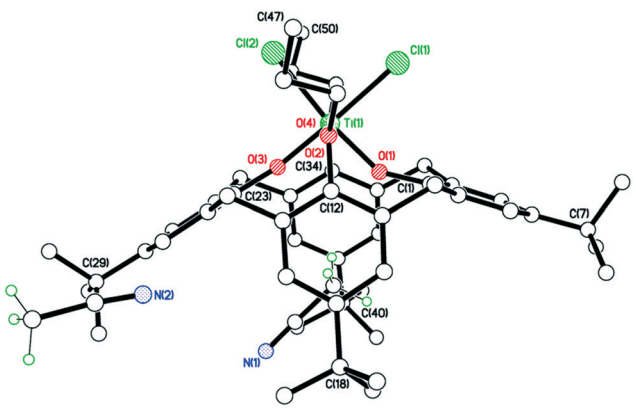

Fig. 1 Molecular structure of $[TiCl_2(L(O)_2(On\text{-}Pr)_2)]\cdot 2MeCN$ (**2**·2MeCN) (most H atoms are omitted for clarity). Selected bond lengths (Å) and angles (°): Ti(1)–Cl(1) 2.3567(5), Ti(1)–Cl(2) 2.3532(5), Ti(1)–O(1) 1.8141(12), Ti(1)–O(2) 2.1193(13), Ti(1)–O(3) 1.7883(12), Ti(1)–O(4) 2.1301(12); Ti(1)–O(1)–C(1) 148.91(11), Ti(1)–O(2)–C(12) 115.31(10), Ti(1)–O(3)–C(23) 171.63(11), Ti(1)–O(4)–C(34) 115.70(10), Cl(1)–Ti(1)–Cl(2) 86.794(18).

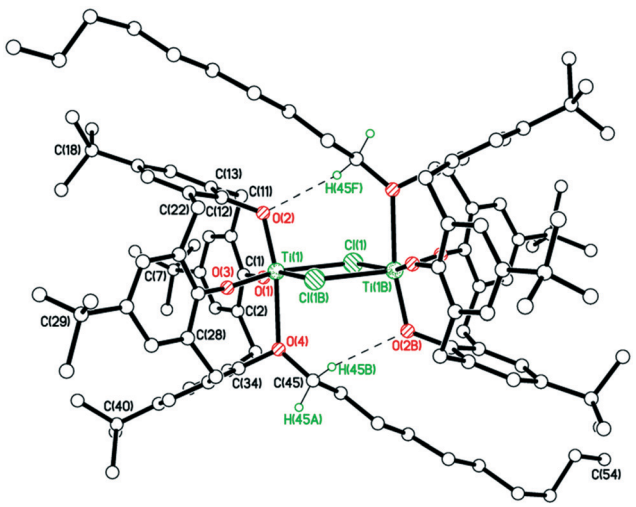

Fig. 2 Molecular structure of $\{[TiL(O)_3(OR)]_2(\mu\text{-}Cl)_2\}\cdot 6MeCN$ (R = *n*-decyl (**4**·6MeCN)) (most H atoms and solvent molecules are omitted for clarity). Selected bond lengths (Å) and angles (°): Ti(1)–Cl(1) 2.4454(12), Ti(1)–Cl(1B) 2.5257(10), Ti(1)–O(1) 1.794(2), Ti(1)–O(2) 1.825(3), Ti(1)–O(3) 1.792(3), Ti(1)–O(4) 2.390(3); Ti(1)–O(1)–C(1) 161.5(2), Ti(1)–O(2)–C(12) 121.9(2), Ti(1)–O(3)–C(23) 158.1(3), Ti(1)–O(4)–C(34) 115.0(2), Cl(1)–Ti(1)–Cl(1B) 77.04(4).

Open Access Article. Published on 27 2020. Downloaded on 10-11-2024 06:39:06.
This article is licensed under a Creative Commons Attribution 3.0 Unported Licence.

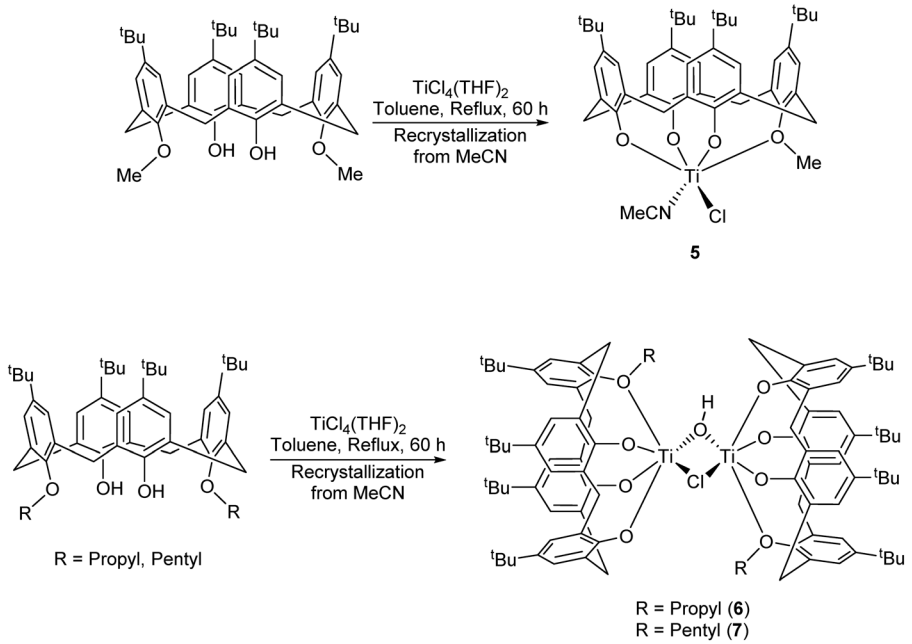

Scheme 2 Synthesis of complexes **5**–**7**.[13]

of the elimination products, namely the non-volatile liquids *n*-propylchloride and *n*-pentylchloride *versus* gaseous CH_3Cl. Instead, in the case of R = *n*-propyl, a dimeric Ti_2 complex showing calix[4]arene moieties bearing only one *n*-propyl substituent each was isolated. Given the two Ti atoms are connected by Cl^- and OH^- bridges, it was hypothesized that the complex arose by adventitious exposure to air during work-up of the parental dichloride complex **2**. The molecular structure of {[TiL(O)$_3$(O*n*-Pr)]$_2$(μ-Cl)(μ-OH)}·7MeCN (**6**·7MeCN) (CCDC 1954695) is shown in Fig. 4 with selected bond lengths and angles given in the caption. The dimeric structure exhibits the previously seen bridging OH^-/Cl^- motif,[14] linking the two distorted octahedral titanium centers. The calixarenes each adopt a 'down, down, down, out' conformation.

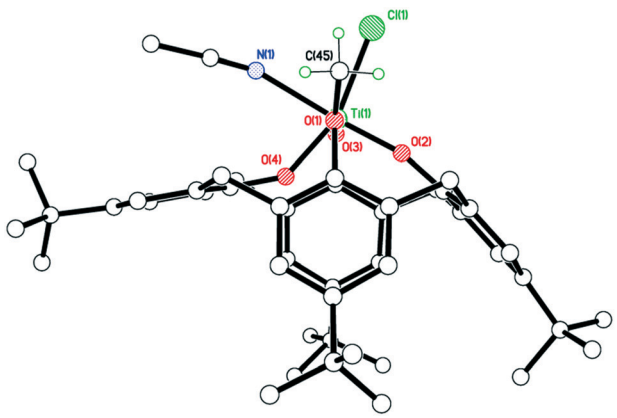

Fig. 3 Molecular structure of [Ti(NCMe)Cl(L(O)$_3$(OR))]·MeCN (**5**·MeCN) (most H atoms and solvent molecules are omitted for clarity). Selected bond lengths (Å) and angles (°): Ti(1)–O(1) 2.3275(11), Ti(1)–O(2) 1.7831(12), Ti(1)–O(3) 1.8500(12), Ti(1)–O(4) 1.8607(12), Ti(1)–N(1) 2.2633(16), Ti(1)–Cl(1) 2.3328(5); O(1)–Ti(1)–O(3) 167.56(5), O(2)–Ti(1)–O(4) 101.81(5), Cl(1)–Ti(1)–N(1) 80.47(4), Ti(1)–O(1)–C(1) 116.05(9), Ti(1)–O(2)–C(12) 163.56(11), Ti(1)–O(3)–C(23) 120.71(9), Ti(1)–O(4)–C(34) 141.47(10).

In the case of R = *n*-pentyl, the complex isolated was identified as {[TiL(O)$_3$(O*n*-pentyl)]$_2$(μ-Cl)(μ-OH)}·7.5MeCN (**7**·7.5MeCN). The molecular structure (CCDC 1954696) is shown in Fig. 5, with selected bond lengths and angles given in the caption. Each titanium center is distorted octahedral with the coordinated provided by a mono-pentoxy calix[4]arene and bridging hydroxyl and chloro ligation. In the packing, the calixarene cavities approach each other forming fairly large solvent accessible volumes, leading to the observed disorder in the MeCN of crystallization.

This type of reaction was further complicated when [TiCl$_4$(THF)$_2$] was employed as the metal precursor.[15] In this case, on attempting to isolate the *n*-propyl analogue of **5**, the orange/red co-crystallized complex [Ti(NCMe)(μ$_3$-O)L(O)$_4$TiCl(O(CH$_2$)$_4$Cl)]$_2$–2[TiCl(NCMe)(L(O)$_3$(O*n*-Pr))]·11MeCN (**8**·11MeCN) was isolated in moderate yield. The molecular structure (CCDC 1954697) is shown in Fig. 6, with selected bond lengths and angles given in the caption. The asymmetric unit comprises half a tetrametallic complex, one monometallic complex and 5.5 MeCNs. The tetrametallic complex lies on a centre of symmetry, with octahedral metal centres bound by either a calix[4]arene which adopts a cone conformation with a metal-bound MeCN in the cavity and a μ$_3$-oxo {Ti(2) and Ti(2A)}, or in the case of Ti(3) and Ti(3A) by an oxygen from each L, the two μ$_3$-oxos and a chlorinated butoxy ligand (O(CH$_2$)$_4$Cl). The calix[4]arenes have lost all of their lower rim bound *n*-propyl groups. By contrast, in the monometallic complex, the calixarene adopts a 'down, down, down, out' conformation and retains an *n*-propyl group.

This journal is © The Royal Society of Chemistry 2020

Open Access Article. Published on 27 2020. Downloaded on 10-11-2024 06:39:06.
This article is licensed under a Creative Commons Attribution 3.0 Unported Licence.

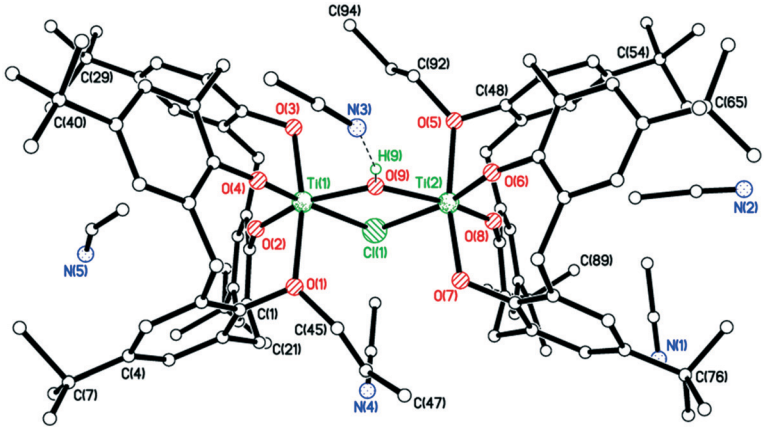

Fig. 4 Molecular structure of {[TiL(O)$_3$(O*n*-propyl)]$_2$(μ-Cl)(μ-OH)}·7MeCN (**6**·7MeCN) (H atoms and two solvent molecules are omitted for clarity). Selected bond lengths (Å) and angles (°): Ti(1)–O(1) 2.191(3), Ti(1)–O(2) 1.818(3), Ti(1)–O(3) 2.004(3), Ti(1)–O(4) 1.780(3), Ti(1)–O(9) 1.979(2), Ti(1)–Cl(1) 2.5167(10); O(1)–Ti(1)–O(3) 168.71(10), O(2)–Ti(1)–O(4) 104.92(12), Cl(1)–Ti(1)–O(9) 74.12(8), Ti(1)–O(1)–C(1) 116.0(2), Ti(1)–O(2)–C(12) 148.8(2), Ti(1)–O(3)–C(23) 118.7(2), Ti(1)–O(4)–C(34) 167.7(2).

We have also investigated the air/water stability of a number of these systems, given that often during catalysis small amounts of water are present, which can lead to often unwanted transesterification processes. Furthermore, studies have revealed that the water content of hydrophilic monomers such as ε-CL can varying greatly with temperature and time.[16] Thus, given the likely presence of water in our ROP studies, we re-visited the type I complex with R = *n*-pentyl, for which we had previously structurally characterized the complex {[TiL(O)$_3$(OR)]$_2$(μ-Cl)(μ-OH)}·7*1*/4MeCN, as well as the and *n*-decyl system.[14] Following initial exposure to air (2 h), work-up was conducted under an inert atmosphere of nitrogen (Scheme 3a). In the case of R = *n*-pentyl, the complex isolated, namely {[TiL(O)$_3$(O*n*-pentyl)]$_2$(μ-Cl)(μ-OH)}·9MeCN **9**·9MeCN, differed only in the degree of solvation from 7·7.5MeCN and from that which we reported previously, see ESI,† Fig. S2 (CCDC 1954689); all geometrical parameters were very similar.

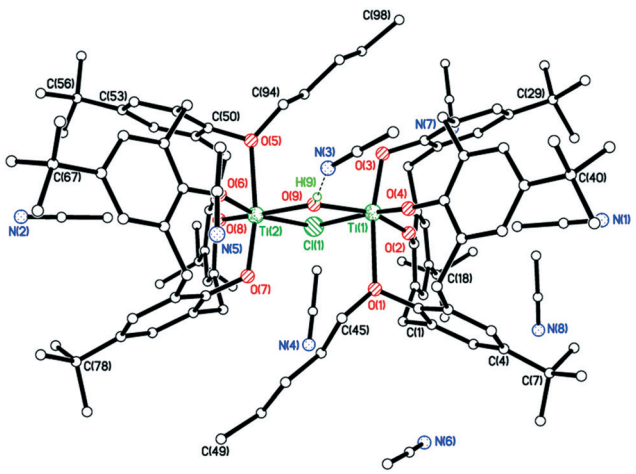

Fig. 5 Molecular structure of {[TiL(O)$_3$(O*n*-pentyl)]$_2$(μ-Cl)(μ-OH)}·7.5MeCN (**7**·7.5MeCN) (most H atoms are omitted for clarity). Selected bond lengths (Å) and angles (°): Ti(1)–O(1) 2.342(2), Ti(1)–O(2) 1.815(2), Ti(1)–O(3) 1.880(2), Ti(1)–O(4) 1.786(2), Ti(1)–O(9) 1.991(2), Ti(1)–Cl(1) 2.5128(8); O(1)–Ti(1)–O(3) 169.08(8), O(2)–Ti(1)–O(4) 104.48(9), Cl(1)–Ti(1)–O(9) 74.02(6), Ti(1)–O(1)–C(1) 114.29(16), Ti(1)–O(2)–C(12) 149.03(17), Ti(1)–O(3)–C(23) 119.70(17), Ti(1)–O(4)–C(34) 165.2(2).

In the case of the *n*-decyl system, crystallization from acetonitrile again afforded a chloro/hydroxyl-bridged complex, namely {[TiL(O)$_3$(O*n*-decyl)]$_2$(μ-Cl)(μ-OH)}·8.5MeCN (**10**·8.5MeCN). The molecular structure (CCDC 1954690) of **10**·8.5MeCN is shown in Fig. 7, with selected bond lengths and angles given in the caption; alternative views are given in the ESI† (Fig. S3). Each titanium is distorted octahedral, and is bound by a calix[4]arene ligand bearing only one decyl chain. One decyl chain, on O(1), is fully extended, but the other, on O(5), is only straight until the 6th C atom, at which point it is somewhat folded. Molecules of **10** pack into layers in the *b*/*c* plane, but are generally well-separated with MeCNs of crystallization in crevices between molecules. MeCNs at N(3), N(7) and N(10) reside mostly with the calixarene cavities and with Me groups furthest inside, the others lie *exo*.

We observed that if the entire procedure above was conducted in air, then the result was precipitation of the parent calixarene ligand. However, we found that conducting a controlled hydrolysis reaction of the type I complex with R = *n*-pentyl, *i.e.* addition of 0.5 equivalents of H_2O to a toluene solution of [TiCl$_2$L(O)$_2$(O*n*-pentyl)$_2$] under reflux, followed by extraction into acetonitrile and then crystallization (still under nitrogen) led to the isolation of orange, plate-like crystals in moderate yield (Scheme 3b). The molecular structure (see Fig. 8) revealed a co-crystallized species (**11**).

One Ti_2 complex plus half the non-coordinated co-crystallized bis-*n*-pentyl ligand, plus the solvent of crystallization in the asymmetric unit (CCDC 1954691). Each Ti adopts a distorted octahedral conformation. The bis-*n*-pentyl ligand lies on a center of symmetry at the body center of the unit cell. The non-coordinated calix[4]arene molecule retains two phenol hydrogens which form intramolecular

Open Access Article. Published on 27 2020. Downloaded on 10-11-2024 06:39:06.
This article is licensed under a Creative Commons Attribution 3.0 Unported Licence.

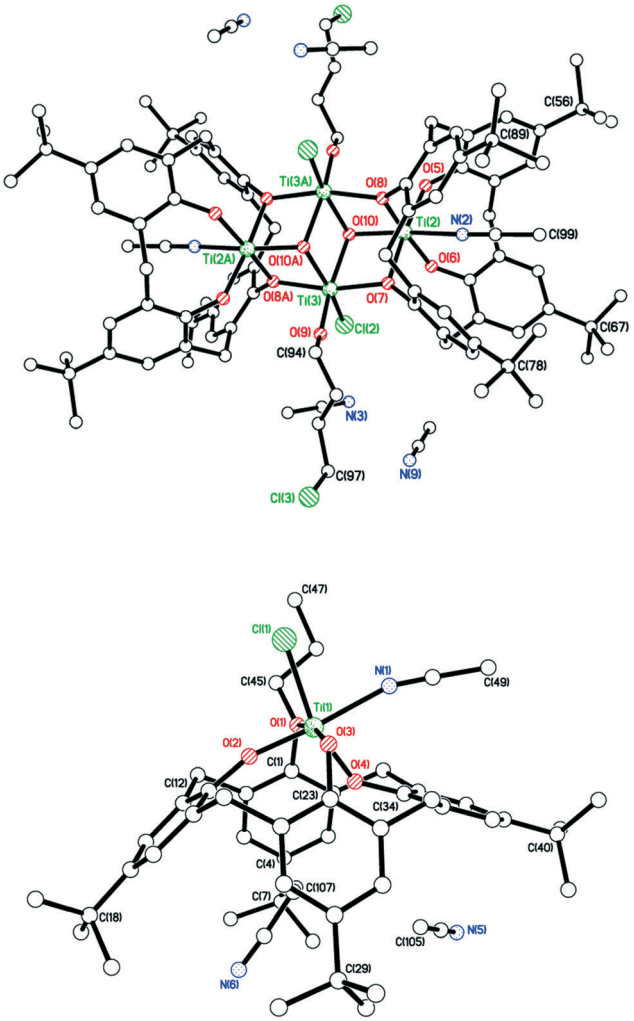

Fig. 6 Molecular structure of $[Ti(NCMe)(\mu_3\text{-}O)L(O)_4TiCl(O(CH_2)_4Cl)]_2$–2[TiCl(NCMe)(L(O)$_3$(O*n*-Pr))]·11MeCN (**8**·11MeCN) (H atoms and some solvent molecules are omitted for clarity). Selected bond lengths (Å) and angles (°): Ti(1)–O(1) 2.3307(19), Ti(1)–O(2) 1.7892(19), Ti(1)–O(3) 1.8406(18), Ti(1)–O(4) 1.8534(19), Ti(1)–N(1) 2.234(2), Ti(1)–Cl(1) 2.3363(8), Ti(2)–O(5) 1.8362(17), Ti(2)–O(6) 1.8321(17), Ti(2)–O(7) 2.0607(16), Ti(2)–O(8) 2.0497(16), Ti(2)–O(10) 1.8463(17), Ti(2)–N(2) 2.207(2), Ti(3)–O(7) 1.9800(17), Ti(3)–O(9) 1.855(2), Ti(3)–O(10) 2.0834(17), Ti(3)–O(8A) 2.0216(17), Ti(3)–O(10A) 2.0139(17), Ti(3)–Cl(2) 2.2999(7); O(1)–Ti(1)–O(3) 168.80(8), O(2)–Ti(1)–O(4) 102.23(9), Ti(1)–O(1)–C(1) 115.47(15), Ti(1)–O(2)–C(12) 162.29(19), Ti(1)–O(3)–C(23) 120.39(15), Ti(1)–O(4)–C(34) 142.39(16).

H-bonds to the neighbouring oxygens. This molecule adopts a 1,2-alternate conformation. The existence of the co-crystallized bis-*n*-pentyl ligand demonstrates that this is the species added to the reaction and that the loss of one *n*-pentyl group occurs upon coordination. The coordinated calix[4]arenes are essentially eclipsed when the complex molecule is viewed end-on (see Fig. S4, ESI†).

For catalytic comparison purposes, a titanium complex $\{TiCl_2(2,2'\text{-}CH_3CH[4,6\text{-}(t\text{-}Bu)_2C_6H_2O]_2)\}$ (**12**) bearing a di-phenolate ligand derived from the diphenol $2,2'\text{-}CH_3CH[4,6\text{-}(t\text{-}Bu)_2C_6H_2OH]_2$ was synthesized according to the procedure reported by Aida *et al.* (Scheme 4).

Plate-like, orange crystals suitable for X-ray analysis were obtained from a saturated hexane solution of the complex upon standing at room temperature for 2 days. The molecular structure of **12** (CCDC 969053) is shown in Fig. 9. A tetrahedral Ti^{4+} is coordinated to two chlorides and two di-phenolate oxygens. The complex is chiral but only one enantiomer is present. The fold angle between rings C(1) > C(6) and C(17) > C(22) is 64.63(7)°. No disorder or solvent of crystallization are observed.

ROP screening

ε-Caprolactone (ε-CL)

We have examined the ability of the complexes prepared herein to act as catalysts for the ROP of ε-CL both under nitrogen and in air; the ROP of ε-CL under air when using the titanium tetraalkoxides $Ti(Oi\text{-}Pr)_4$ and $Ti(On\text{-}Bu)_4$ has been reported.[16]

Firstly, looking at the series $[TiCl_2L(O)_2(OR)_2]$ (type I: R = Me (**1**), *n*-Pr (**2**) and *n*-pentyl (**3**)), at 130 °C over 24 h with a ratio of 500 : 1 and in the presence of two equivalents of benzyl alcohol, all three are efficient catalysts and afford >99% conversion (runs 1–4, Table 1). Complex **1** as its MeCN solvate exhibits the best control, whilst in all cases, observed molecular weights are far lower than calculated values suggesting extensive transesterification is occurring (Scheme 5).[8] Over 1 h (runs 5–7), some differentiation is possible with highest conversion achieved using the pentyl catalyst system **3**. Interestingly, if the ROP runs are conducted under air (runs 8–10), the catalysts remain efficient with conversions >99%, with comparable molecular weights for the polymers isolated using **1** and **2** as those obtained under N_2, though that from **3** was somewhat lower.

The control in air was generally better than that observed under N_2. On lowering the temperature to 80 °C, over 24 h (runs 14–16), complex **3** was again the most active, with both systems **1** and **3** affording polymers with good control (M_w/M_n = 1.1). In the case of system **2**, only oily oligomers were isolated (360 Da). Over 1 h at 80 °C (runs 20–22), the systems were inactive. When runs were conducted in the absence of benzyl alcohol (runs 29–31), all systems were again active (>99% conversion), with observed molecular weight higher than for comparable runs in the presence of external alcohol. This could be ascribed to the lack of the chain-transfer to the co-activator (see Scheme 5). Over 1 h at 130 °C in the absence of alcohol, the systems were inactive (runs 26–28). It was noteworthy that complete conversion was achieved in the ROP conducted in air in the presence of complex **4**·MeCN (run 11). The same outcome was achieved at 80 °C over 24 h (run 17). Although only 11% conversion was obtained after 1 h (run 17), the complex proved to be more active than its congeners **1**–**3**.

Screening of the complex [Ti(NCMe)Cl(L(O)$_3$(OMe))]·MeCN (**5**·MeCN) under the same conditions employed for **1**–**3** revealed that this system was more active, for example over 1 h, conversions were >85% in air (run 13), whilst at 80 °C over

 This journal is © The Royal Society of Chemistry 2020

Open Access Article. Published on 27 2020. Downloaded on 10-11-2024 06:39:06.
This article is licensed under a Creative Commons Attribution 3.0 Unported Licence.

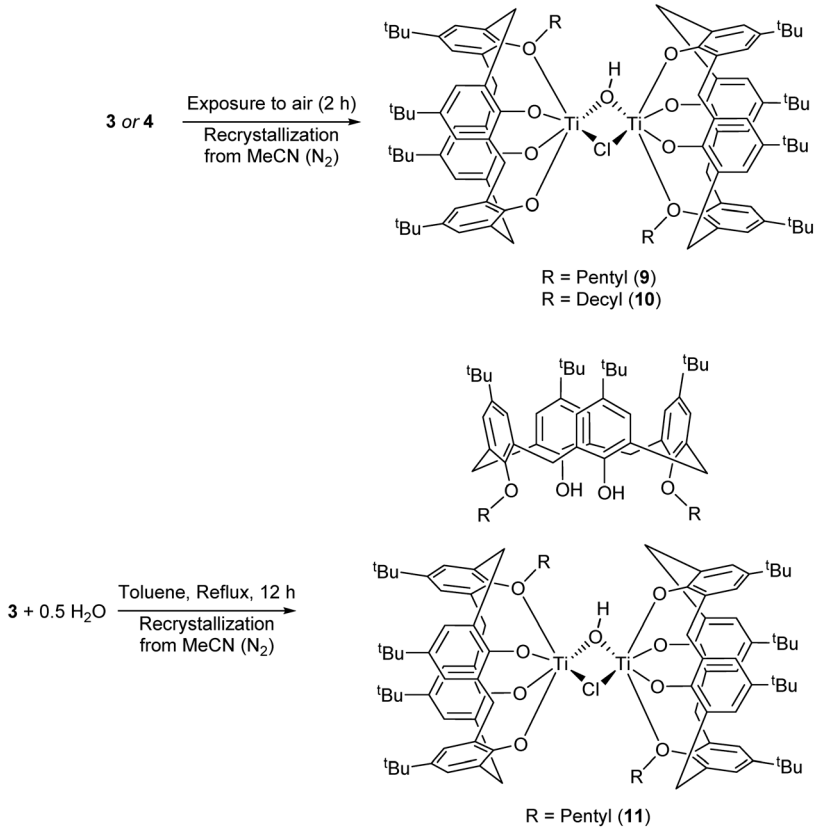

Scheme 3 Formation of compounds **9**–**11** from the parental complexes **3** and **4**.

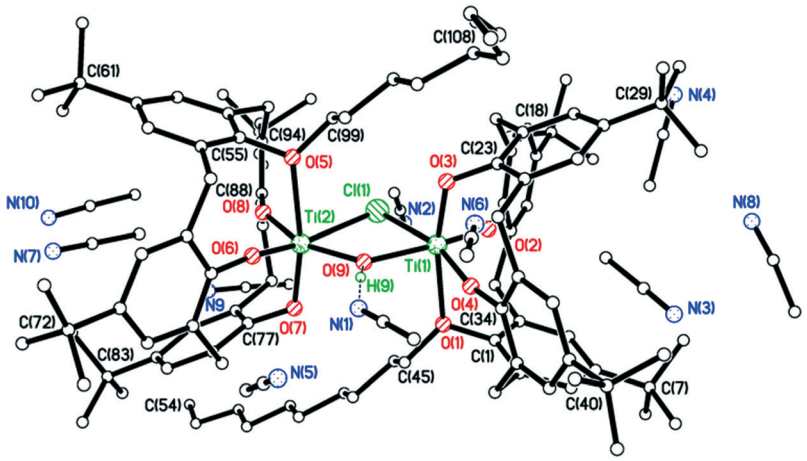

Fig. 7 Molecular structure of {[TiL(O)$_3$(O*n*-decyl)]$_2$(μ-Cl)(μ-OH)}·8.5MeCN (**10**·8.5MeCN) (most H atoms are omitted for clarity). Selected bond lengths (Å) and angles (°): Ti(1)–O(1) 2.381(3), Ti(1)–O(2) 1.817(3), Ti(1)–O(3) 1.852(3), Ti(1)–O(4) 1.793(3), Ti(1)–O(9) 2.000(3), Ti(1)–Cl(1) 2.5177(14); O(1)–Ti(1)–O(3) 168.54(13), O(2)–Ti(1)–O(4) 102.84(15), Cl(1)–Ti(1)–O(9) 74.82(10), Ti(1)–O(1)–C(1) 112.8(2), Ti(1)–O(2)–C(12) 150.5(3), Ti(1)–O(3)–C(23) 119.9(2), Ti(1)–O(4)–C(34) 168.3(3).

24 h under N_2 (runs 18, 19) conversions were >99% and over 1 h (run 24) conversions were >37%.

The analysis of the polymer terminal groups was performed by means of ^{1}H NMR spectroscopy. The spectra of the PCLs synthesized in the presence of the co-activator, both under nitrogen and in air, exhibited signals for the aromatic and benzylic protons of the benzyloxy-end group (δ = 7.35 and 5.10 ppm, respectively) in a 5 : 2 ratio (see the ESI,† Fig. S5 and S6, respectively). As expected, such signals were not observed in the spectrum of the polymer isolated in the absence of benzyl alcohol (see the ESI,† Fig. S7). In all cases, the triplet corresponding to the terminal –CH_2OH group (δ = 3.65 ppm) was also observed. For the polymers isolated with BnOH, the ratio between the areas of the benzyl- and –CH_2OH groups was found to be far from the theoretical value (5 : 2 : 2 *vs.* 5 : 2 : 6 and 5 : 2 : 10 for the run under N_2 and air,

Open Access Article. Published on 27 2020. Downloaded on 10-11-2024 06:39:06.
This article is licensed under a Creative Commons Attribution 3.0 Unported Licence.

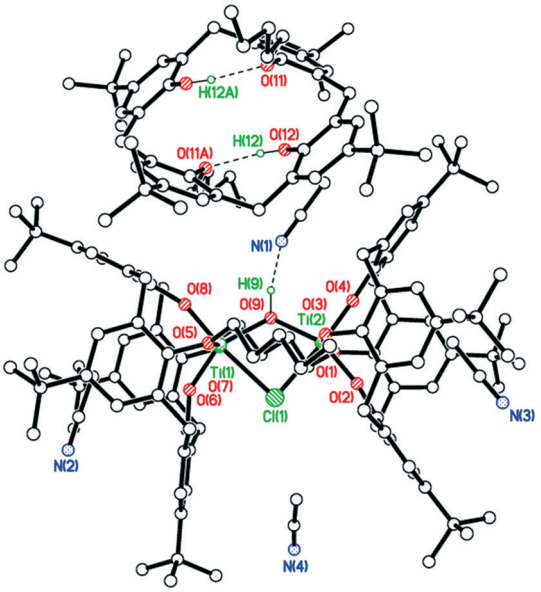

Fig. 8 Molecular structure of $[Ti_2(OH)Cl(L(O)_3(OR))][L(OH)_2(OR)_2]\cdot 2.85(MeCN)\cdot 0.43(H_2O)$ (**11**) (most H atoms are omitted for clarity). Selected bond lengths (Å) and angles (°): Ti(1)–O(5) 2.396(2), Ti(1)–O(6) 1.8106(19), Ti(1)–O(7) 1.839(2), Ti(1)–O(8) 1.804(2), Ti(1)–O(9) 1.975(4), Ti(1)–Cl(1) 2.6141(18); Ti(1)–O(5)–C(50) 114.99(16), Ti(1)–O(6)–C(61) 149.3(2), Ti(1)–O(7)–C(72) 121.78(18), Ti(1)–O(8)–C(83) 157.3(2), Cl(1)–Ti(1)–O(9) 70.75(13), Ti(1)–Cl(1)–Ti(2) 88.10(6), Ti(1)–O(9)–Ti(2) 126.0(2).

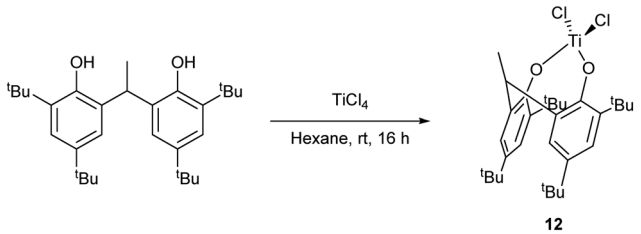

Scheme 4 Synthesis of the di-phenolate complex **12**.[17]

respectively). This could be ascribed to the broad dispersities of the samples and/or to the formation of cyclic oligomers. Hence, further identification of end groups *via* MALDI-TOF mass spectrometry was undertaken. For the PCL isolated in the presence of BnOH under inert atmosphere (see the ESI,† Fig. S8), a main population compatible with benzyl- and CH_2-OH terminated polymers was observed; this was consistent with the ^{1}H NMR spectrum of the sample. Nevertheless, a second distribution ascribable to cyclic compounds was also identified. In the case of the sample obtained in aerobic conditions, only cyclic species were observed for low M_n (20–30 repeating units, see the ESI,† Fig. S9a). For higher molecular weights (>35 repeating units), a second distribution accountable to α-hydroxyl-ω-(carboxylic acid) poly(ε-caprolactones) was detected (see the ESI,† Fig. S9b and c). For higher fractions, such distribution became predominant, although cyclic species are still present. The formation of α-hydroxyl-terminated chains could be explained considering that the insertion of the first monomer unit into a Ti–OH bond arises from the reaction of the pre-

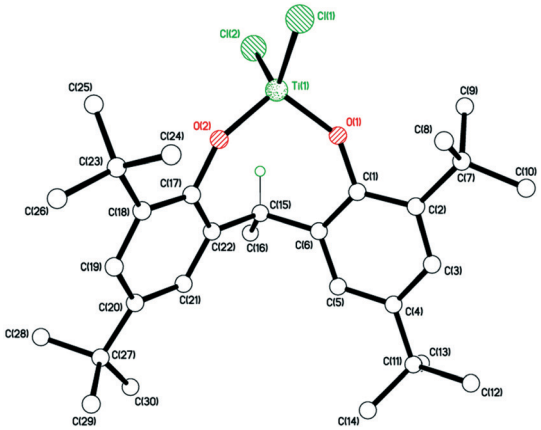

Fig. 9 Molecular structure of {$TiCl_2$(2,2′-CH3CH[4,6-(*t*-Bu)2C6H2O]2)} (**12**) (most H atoms are omitted for clarity). Selected bond lengths (Å) and angles (°): Ti(1)–O(1) 1.7593(15), Ti(1)–O(2) 1.7559(14), Ti(1)–Cl(1) 2.2209(6), Ti(1)–Cl(2) 2.2284(7); C(1)–O(1)–Ti(1) 145.96(13), C(17)–O(2)–Ti(1) 151.26(13), O(2)–Ti(1)–Cl(2) 110.27(6), O(1)–Ti(1)–Cl(1) 109.15(5), O(2)–Ti(1)–O(1) 105.38(7).

catalyst (or its parental benzyloxy-derivative) with adventitious water.[18] Similarly, only cyclic species were observed in the polymer isolated in the absence of BnOH for low M_n (17–24 repeating units, see ESI,† Fig. S10a). Noteworthy, the formation of cyclic polyesters occurring in the absence of BnOH has recently been reported.[19] A distribution of α-hydroxyl-ω-(carboxylic acid)-terminated polymers became predominant for higher fractions (see ESI,† Fig. S10b and c). Interestingly, no Cl-terminal groups were detected, suggesting the inability of the Ti–Cl species to promote ROP reactions.[17,18] Also in this case, the active species was thought to be a Ti–OH compound derived from the hydrolysis of the pre-catalyst.

δ-Valerolactone (δ-VL)

For the ROP of δ-VL (Table 2), using **1–3**, at 80 °C over 24 h (runs 1–3) only moderate activity was observed with conversions ≤50% (activity followed the trend **1** > **2** > **3**), but with good control and observed molecular weights much lower than calculated values. Higher conversion (78%) was obtained in the presence of **4** (run 4). Interestingly, the molecular weight observed was close to the calculated value. In the case of the reaction performed over 1 h at 80 °C, systems **1–3** were inactive, while only 4% conversion was observed with complex **4** (runs 7–9 and 10, respectively). In the case of [Ti(NCMe)Cl(L(O)$_3$(OMe))]·MeCN (**5**·MeCN), good activity (81% conversion) was observed at 80 °C in the presence of either one or two equivalents of BnOH over 24 h (runs 5 and 6). Over 1 h, **5**·MeCN exhibited low activity ≤14%. Moderate activity (62% conversion) was also observed on conducting the reaction under air over 24 h (run 7). Also in this case, the ^{1}H NMR spectra of selected polymer samples highlighted the presence of benzyl- and –CH_2OH terminal groups (see the ESI,† Fig. S11 and S12, for the run performed under N_2 and in air, respectively).

This journal is © The Royal Society of Chemistry 2020

Open Access Article. Published on 27 2020. Downloaded on 10-11-2024 06:39:06.
This article is licensed under a Creative Commons Attribution 3.0 Unported Licence.

Table 1 ROP of ε-CL

Run	Catalyst/solvent	ε-CL : M : BnOH	T (°C)	t (h)	Conv.[a] (%)	$M_{n(obs)}$[b]	$M_{n(corr)}$[c]	$M_{n(calc)}$[d]	M_w/M_n[b]
1	**1 Tol**	500 : 1 : 2	130	24	>99	5390	3020	28 360	2.90
2	**1 MeCN**	500 : 1 : 2	130	24	>99	7330	4100	28 360	1.30
3	**2 MeCN**	500 : 1 : 2	130	24	>99	13 710	7680	28 360	2.20
4	**3 MeCN**	500 : 1 : 2	130	24	>99	9280	5200	28 360	2.40
5	**1 MeCN**	500 : 1 : 2	130	1	2	nd	nd		nd
6	**2 MeCN**	500 : 1 : 2	130	1	3	nd	nd		nd
7	**3 MeCN**	500 : 1 : 2	130	1	12	nd	nd		nd
8[e]	**1 MeCN**	500 : 1 : 2	130	24	>99	6390	3580	28 360	1.80
9[e]	**2 MeCN**	500 : 1 : 2	130	24	>99	6060	3390	28 360	1.40
10[e]	**3 MeCN**	500 : 1 : 2	130	24	>99	2910	1630	28 360	1.50
11[e]	**4 MeCN**	500 : 1 : 2	130	24	>99	20 930	11 770	28 360	2.47
12[e]	**5 MeCN**	500 : 1 : 2	130	24	>99	8180	4580	28 360	2.08
13[e]	**5 MeCN**	500 : 1 : 2	130	1	85	19 130	10 710	24 350	1.82
14	**1 MeCN**	500 : 1 : 2	80	24	32	6510	3650	9240	1.10
15	**2 MeCN**	500 : 1 : 2	80	24	33	650	360	9240	1.06
16	**3 MeCN**	500 : 1 : 2	80	24	68	6310	3640	19 510	1.10
17	**4 MeCN**	500 : 1 : 2	80	24	>99	33 990	19 030	28 360	1.55
18	**5 MeCN**	500 : 1 : 2	80	24	>99	16 530	9260	28 360	1.48
19	**5 MeCN**	500 : 1 : 1	80	24	>99	14 470	8100	28 360	1.40
20	**1 MeCN**	500 : 1 : 2	80	1	None	—	—		—
21	**2 MeCN**	500 : 1 : 2	80	1	None	—	—		—
22	**3 MeCN**	500 : 1 : 2	80	1	None	—	—		—
23	**4 MeCN**	500 : 1 : 2	80	1	11				
24	**5 MeCN**	500 : 1 : 2	80	1	37				
25	**5 MeCN**	500 : 1 : 1	80	1	11				
26	**1 MeCN**	500 : 1 : 0	130	1	None	—	—		—
27	**2 MeCN**	500 : 1 : 0	130	1	None	—	—		—
28	**3 MeCN**	500 : 1 : 0	130	1	None	—	—		—
29	**1 MeCN**	500 : 1 : 0	130	24	>99	13 740	7690	28 360	1.40
30	**2 MeCN**	500 : 1 : 0	130	24	>99	14 820	8300	28 360	1.90
31	**3 MeCN**	500 : 1 : 0	130	24	>99	18 840	10 550	28 360	1.80

Reaction conditions: toluene 5 mL, [ε-CL] = 0.9 M, N_2. [a] Determined by ^{1}H NMR spectroscopy on crude reaction mixture. [b] From GPC. [c] Values corrected considering Mark–Houwink factor (0.56) from polystyrene standards in THF. [d] Calculated from ($[monomer]_0/[OH]_0$) × conv. (%) × monomer molecular weight + molecular weight of BnOH. [e] Reaction performed in air.

rac-Lactide (*r*-LA)

Attempted polymerization of *r*-LA was less successful. At 80 °C over 24 h, none of the systems proved to be active (runs 1–4, Table 3). On increasing the temperature to 130 °C, almost complete conversion was achieved with complexes **1**–**3** and **5** (runs 5–7 and 9, respectively), while moderate activity was observed in the case of **4** (65% conversion, run 8). In the case of systems **1**–**3** and **5**, the molecular mass observed was lower than the calculated values and there was poor control. It is noteworthy that a monodisperse polymer (M_w/M_n = 1.04) with molecular mass observed close to the calculated value was obtained with complex **4**. It was hypothesized that in the presence of such catalysts, the rate of transesterification processes was lower than that of the chain growth allowing for the occurrence of a living polymerization. By contrast, 1–3 and 5 are subject to increased transesterification *versus* the other systems. Interestingly, complete conversion was achieved in air by using complex **5** (run 10). None of the systems was active over 1 h (runs 11–16). The syndiotactic bias was determined by 2D *J*-resolved ^{1}H NMR spectroscopy, investigating the methine area (*ca.* 5.2 ppm) of the spectra (see ESI,† Fig. S13–S17).[20] The peaks were assigned to the corresponding tetrads according to the literature reports.[21] While complexes **1** and **2** afforded almost heterotactic polymers (P_r 0.46 and 0.42, respectively), isotactic materials were isolated in the case of systems **3**, **4**, and **5** (Chart 2).

ω-pentadecalactone (ω-PDL)

In the case of the larger cyclic ester ω-PDL, only catalyst **5** was successful, achieving moderate activity at 130 °C over 24 h (run 1, Table 4). Low activity (11% conversion) was observed when the reaction was carried out in air (run 3, Table 4). In both cases, molecular weights lower than the expected values and compatible with oligomeric species (12–13 units) were observed. Also in this case, the benzyl end-group was observed by ^{1}H NMR spectroscopy on the polymer sample (see the ESI,† Fig. S18).

Interestingly, the triplet corresponding to the –CH_2OH group was not observed. However, a rigorous analysis of the terminal groups could not be performed due the presence of the signals of residual monomer which could not be separated from the polymer.

Open Access Article. Published on 27 2020. Downloaded on 10-11-2024 06:39:06.
This article is licensed under a Creative Commons Attribution 3.0 Unported Licence.

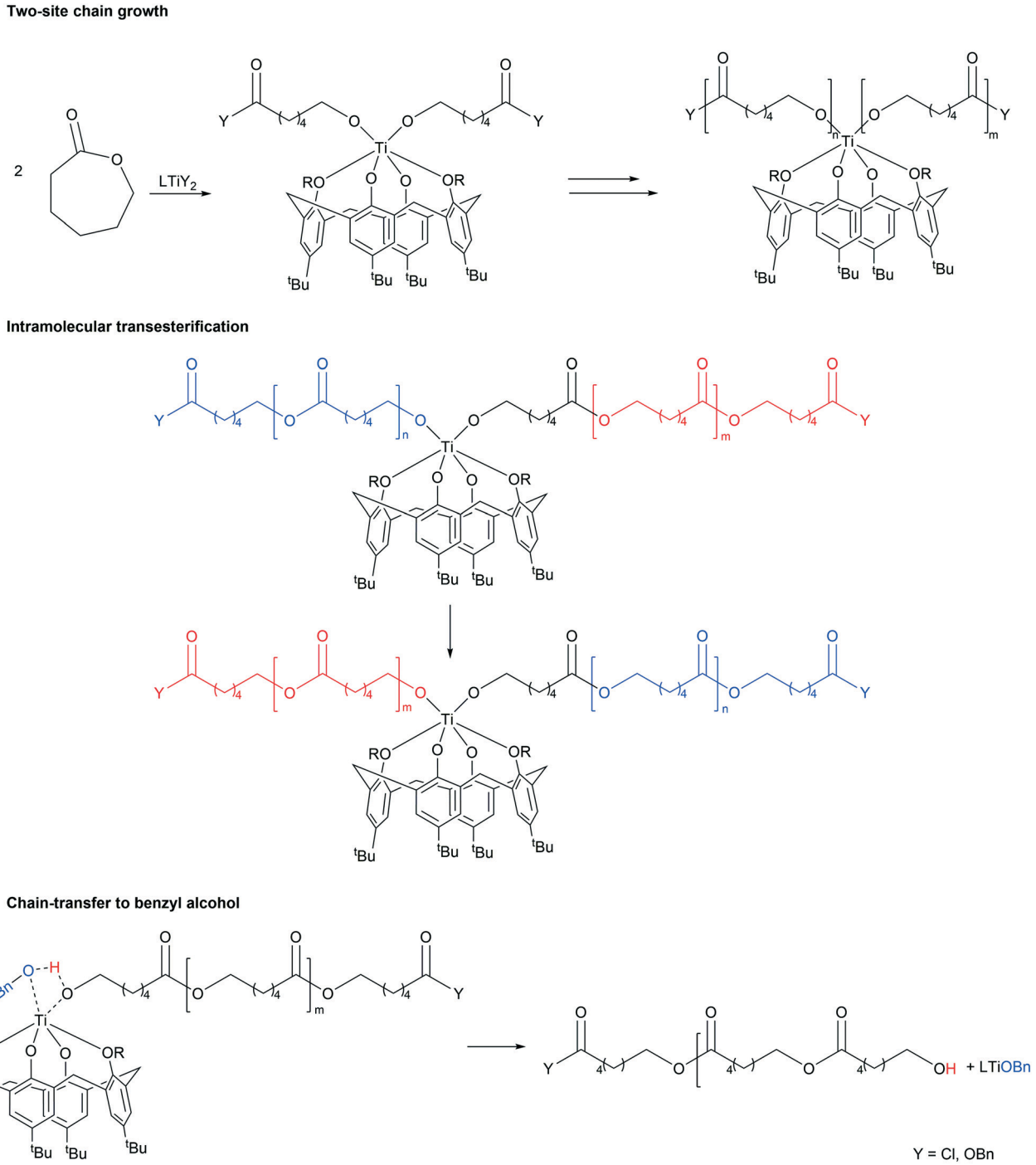

Scheme 5 Proposed pathways for chain-growth, intramolecular transesterification and chain-transfer to co-catalyst [adapted from ref. 8].

Co-polymerization of ε-CL with δ-VL

At 80 °C using **5**, high activity (99% conversion) was observed over 24 h affording a polymer of molecular weight >23 000 Da (Table 5, run 1). The ratio CL/VL was found to be 1 : 1, as highlighted by ^{1}H NMR spectroscopy (see the ESI,† Fig. S19). Interestingly, a similar outcome was observed in the case of the reaction performed in air at higher temperature (Table 5, entry 3). A broadening of the molecular weight distribution was also detected (2.26 *vs.* 1.30). The composition of the co-polymer was further investigated by ^{13}C NMR spectroscopy. In fact, diagnostic resonances belonging to CL–VL, CL–CL, VL–VL and VL–CL dyads can be observed in the region between 63.7 and 64.5 (see ESI,† Fig. S20).[22] Based in the integrations of these signals, the number-average sequence length was found to be 2.22 and 1.82 for CL and VL, respectively, compatible with a "random-type" co-polymer (randomness degree, R = 0.90, see ESI,† eqn (S1)–(S3)). The thermal properties of the co-

 This journal is © The Royal Society of Chemistry 2020

Open Access Article. Published on 27 2020. Downloaded on 10-11-2024 06:39:06.
This article is licensed under a Creative Commons Attribution 3.0 Unported Licence.

Table 2 ROP of δ-VL

Run	Catalyst/solvent	δ-VL : Ti : BnOH	T (°C)	t (h)	Conv.[a] (%)	M_n[b]	$M_{n(calc)}$[c]	M_w/M_n[b]
1	**1 MeCN**	500 : 1 : 2	80	24	50	5310	12 620	1.10
2	**2 MeCN**	500 : 1 : 2	80	24	45	6090	11 360	1.13
3	**3 MeCN**	500 : 1 : 2	80	24	44	5700	11 060	1.10
4	**4 MeCN**	500 : 1 : 2	80	24	78	18.830	19 630	1.60
5	**5 MeCN**	500 : 1 : 2	80	24	81	9550	20 380	1.50
6	**5 MeCN**	500 : 1 : 1	80	24	81	12 570	40 650	1.37
7[d]	**5 MeCN**	500 : 1 : 1	130	24	62	9480	15 650	1.45
7	**1 MeCN**	500 : 1 : 2	80	1	None	—		—
8	**2 MeCN**	500 : 1 : 2	80	1	None	—		—
9	**3 MeCN**	500 : 1 : 2	80	1	None	—		—
10	**4 MeCN**	500 : 1 : 2	80	1	4			
11	**5 MeCN**	500 : 1 : 2	80	1	14			
12	**5 MeCN**	500 : 1 : 1	80	1	6			

Reaction conditions: toluene 5 mL, [δ-VL] = 0.9 M, N_2. [a] Determined by ^{1}H NMR spectroscopy on crude reaction mixture. [b] From GPC. [c] Calculated from ([monomer]$_0$/[OH]$_0$) × conv. (%) × monomer molecular weight + molecular weight of BnOH. [d] Reaction performed in air.

Table 3 ROP of *r*-LA

Run	Catalyst/solvent	*r*-LA : Ti : BnOH	T (°C)	t (h)	Conv.[a] (%)	P_r[b]	$M_{n(corr)}$[c,d]	$M_{n(calc)}$[e]	M_w/M_n[c]
1	**1 MeCN**	500 : 1 : 2	80	24	None				
2	**2 MeCN**	500 : 1 : 2	80	24	None				
3	**3 MeCN**	500 : 1 : 2	80	24	None				
4	**5 MeCN**	500 : 1 : 2	80	24	None				
5	**1 MeCN**	500 : 1 : 2	130	24	95	0.46	13 520	34 310	1.68
6	**2 MeCN**	500 : 1 : 2	130	24	97	0.42	11 170	35 030	1.94
7	**3 MeCN**	500 : 1 : 2	130	24	95	0.23	15 770	34 310	2.09
8	**4 MeCN**	500 : 1 : 2	130	24	65	0.27	22 040	23 480	1.04
9	**5 MeCN**	500 : 1 : 1	130	24	97	0.32	28 830	69 950	1.94
10[f]	**5 MeCN**	500 : 1 : 1	130	24	94	0.25	12 200	34 310	1.73
11	**1 MeCN**	500 : 1 : 2	130	1	None	—	—		
12	**2 MeCN**	500 : 1 : 2	130	1	None	—	—		
13	**3 MeCN**	500 : 1 : 2	130	1	None	—	—		
14	**4 MeCN**	500 : 1 : 2	130	1	None				
16	**5 MeCN**	500 : 1 : 1	130	1	5	—	—		

Reaction conditions: toluene 5 mL, [*r*-LA] = 0.9 M, N_2. [a] Determined by ^{1}H NMR spectroscopy on crude reaction mixture. [b] From 2D *J*-resolved 1H NMR spectroscopy. [c] From GPC. [d] Values corrected considering Mark–Houwink factor (0.58) from polystyrene standards in THF. [e] Calculated from ([monomer]$_0$/[OH]$_0$) × conv. (%) × monomer molecular weight + molecular weight of BnOH. [f] Reaction performed in air.

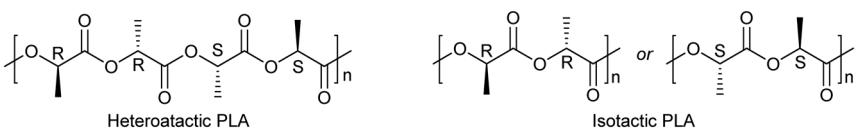

Chart 2 Microstructure of heterotactic and isotactic poly-(*rac*-lactide).[21]

Table 4 ROP of ω-pentadecalactone catalyzed by **5**

Run	ω-PDL : **5** : BnOH	T (°C)	t (h)	Conv.[a] (%)	M_n[b]	$M_{n(calc)}$[c]
1	500 : 1 : 1	130	24	53	2835	63 710
2	500 : 1 : 1	130	1	None	—	—
3[d]	500 : 1 : 1	130	24	11	2600	13 310
4[d]	500 : 1 : 1	130	1	None	—	—

Reaction conditions: toluene 5 mL, [ω-PDL] = 0.9 M, N_2. [a] Determined by ^{1}H NMR spectroscopy on crude reaction mixture. [b] From MALDI-TOF. [c] Calculated from ([monomer]$_0$/[OH]$_0$) × conv. (%) × monomer molecular weight + molecular weight of BnOH. [d] Reaction performed in air.

Table 5 ε-CL/δ-VL co-polymerization

Run	Catalyst/solvent	ε-CL : δ-VL : Ti : BnOH	T (°C)	t (h)	Conv.[a] (%)	M_n[b,c]	M_w/M_n[b]
1	**5 MeCN**	500 : 500 : 1 : 1	80	24	>99	23 350	1.30
2		500 : 500 : 1 : 1	80	1	8.5	—	—
3[d]		500 : 500 : 1 : 1	130	24	>99	28 020	2.26

Reaction conditions: toluene 5 mL, [ε-CL] = [δ-VL] = 0.9 M, N_2. [a] Determined by ^{1}H NMR spectroscopy on crude reaction mixture based on ε-CL. [b] From GPC. [c] Values corrected considering Mark–Houwink factor ($M_n \times 0.56 + M_n$) from polystyrene standards in THF. [d] Reaction performed in air.

Open Access Article. Published on 27 2020. Downloaded on 10-11-2024 06:39:06.
This article is licensed under a Creative Commons Attribution 3.0 Unported Licence.

polymers were studied by DSC (ESI,† Fig. S21). No transitions were observed between 23 and 100 °C, confirming the irregular co-monomer distribution within the polymer chain leading to lower melting points. This is in agreement with the observations recently disclosed by Hu *et al.*[22a]

Co-polymerization of ε-CL with *r*-LA

At 130 °C using **5** and a 10 : 1 ratio of ε-CL/*r*-LA, high activity (99% conversion) was observed over 24 h affording a polymer of molecular weight >5000 Da (Table 6, run 1) which comprised mostly PCL (see the ESI,† Fig. S22). Use of a 1 : 1 ratio of CL/*r*-LA afforded a copolymer of molecular weight >20 500 Da (Table 6, entry 3), for which the ^{1}H NMR spectra indicated only 65% of CL was converted (see the ESI,† Fig. S23). A similar outcome was obtained by performing the reaction in air (Table 6, run 5). The co-polymer compositions was determined by analyzing the carbonyl range of the ^{13}C NMR spectrum.[23] The LA/CL ratio was found to be 75 : 35 and the average sequence length was 3.04 and 2.42 for CL and LA, respectively (ESI,† Fig. S24 and eqn (S3) and (S4)). Noteworthy, no peaks corresponding to the CL–LA–CL triad at 171.1 ppm was observed. Such signals arise from the transesterification of the cleavage of the lactyl–lactyl bond in the lactidyl unit.[23]

Concerning the thermal properties of the co-polymer, no transitions accountable to CL blocks were detected on the DSC curve of the sample (ESI,† Fig. S25). Nevertheless, rather intense endothermic peaks were observed between 150 and 170 °C, suggesting the existence of crystalline PLA-microdomains.[23a]

Comparison with other Ti-based catalysts

Since complex **5** proved to be the most performing catalyst for the ROP of cyclic esters, its activity was compared to that of other Ti-based species, namely the novel di-phenolate complex **12** and the nitro-containing titanocalix[4]arene species cone-5,17-bis-*tert*-butyl-11,23-dinitro-25,27-dipropyloxy-26,28-dioxo-calix[4]arene titanium dichloride **13**, previously reported by Toupet *et al.* (Chart 3).[8]

These complexes, along with [Ti(O*i*-Pr)$_4$] were employed as catalysts in the ROP of different cyclic esters (Table 7). In all cases, **5** outperformed complexes **12** and **13**, both in terms of conversion and polymer M_n (*cf.* for example runs 1–3 and 5–7). Although [Ti(O*i*-Pr)$_4$] was shown to promote the ROP of ε-CL under solvent-free conditions,[16] it was found to be completely inactive under our reaction conditions (toluene, [monomer] = 0.9 M). Notably, only complex **5** proved to be active in the ROP of the larger ω-pentadecalactone.

The polymerization of ε-CL under solvent-free conditions was next considered (Table 8). By performing the reaction in the presence of the monochloride titanocalix[4]arene complex **5**, 50% conversion was achieved within 10 minutes at 80 °C (run 1). Under the same reaction conditions, no reaction was observed neither with the bi-phenolate complex **12** nor with the dichloro-species **13** (runs 2 and 3). Notably, 29% monomer conversion was obtained by using [Ti(O*i*-Pr)$_4$] (run 4). In order to explain the inactivity of **12** and **13**, the inefficient activation of the dichloro-based species in the absence of the solvent was postulated. Differently, the presence of the labile acetonitrile ligand in complex **5** would allow for the prompt formation of the catalytically active species, even under solvent-free conditions. Moreover, higher performance of catalyst **5** over [Ti(O*i*-Pr)$_4$], both in terms of conversion and polymer M_n, highlighted the beneficial effect of the calix[4]arene ligand on the ROP process.

Moreover, the performances of complexes **5**, **12** and **13** were compared in the ROP of ε-CL under aerobic conditions (Table 9). At 130 °C in the presence of **5** and **12**, good and

Table 6 ε-CL/*r*-LA co-polymerization

Run	Catalyst/solvent	ε-CL : *r*-LA : Ti : BnOH	T (°C)	t (h)	Conv.[a] (%)	M_n[b,c]	M_w/M_n[b]
1	**5 MeCN**	500 : 50 : 1 : 1	130	24	>99 (CL)	5190	2.87
2		500 : 50 : 1 : 1	130	1	12 (CL)		
3		500 : 500 : 1 : 1	130	24	>99 (LA)	20 500	2.10
4		500 : 500 : 1 : 1	130	1	47(LA)		
5[d]		500 : 500 : 1 : 1	130	24	>99 (LA)	18 150	2.17

Reaction conditions: toluene 5 mL, [ε-CL] = [*r*-LA] = 0.9 M, N_2. [a] Determined by ^{1}H NMR spectroscopy on crude reaction mixture based on ε-CL. [b] From GPC. [c] M_n values were determined by GPC in THF *vs.* PS standards and were corrected with a Mark–Houwink factor (M_n, GPC × 0.56 × %PCL + M_n, GPC × 0.58 × %Pr-LA). [d] Reaction performed in air.

 This journal is © The Royal Society of Chemistry 2020

Open Access Article. Published on 27 2020. Downloaded on 10-11-2024 06:39:06.
This article is licensed under a Creative Commons Attribution 3.0 Unported Licence.

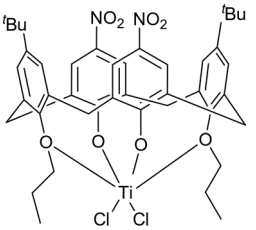

13

Chart 3 Structure of the benchmark Ti-complex **13**.[8]

moderate conversions were obtained within 1 h, respectively (runs 1 and 2). Interestingly, full monomer conversion was observed by performing the reaction with complex **13** (run 3). Nevertheless, higher polymer M_n were achieved in the presence of **5** (19 kDa *vs.* 11 kDa for **5** and **13**, respectively). By carrying out the reaction for 24 h, complete monomer conversion was observed with both **5** and **13** (runs 4 and 5). The M_n of the samples were found to be in a rather narrow range (spanning from 4600 to 5400) albeit better control was exhibited by the monochloride titanocalix[4]arene complex.

Finally, given the interest in metal-free ROP catalysts,[20] the parent 1,3-dialkoxycalixarenes $L(OH)_2(OR)_2$ were also screened under the conditions herein. These metal-free species proved to be inactive.

Kinetics

From a kinetic study of the ROP of ε-CL using **1–5** and **12–13**, it was observed that the polymerization rate exhibited first order dependence on the ε-CL concentration (Fig. 9, left), and the conversion of monomer achieved over 60 min was >75% (100% for **5** and **13**). Fig. 10 indicates that the rate order is **13** > **5** > **12** > **3** > **2** > **1** > **4**. This suggested that a labile acetonitrile ligand (for **5**) or electron-withdrawing groups on the calixarene backbone (for **13**) are beneficial. The induction period of *ca.* 10 min observed for complexes **1–4** could be ascribed to the longer time required for the formation of the catalytically active species (allegedly a Ti-bis(benzyloxide) compound) from a dichloro-precursor.

A kinetic study of the ROP of δ-VL using **1–5** and **12–13**, again revealed first order dependence on the monomer concentration (Fig. 11, left). Conversions over 60 min were lower than observed for ε-CL with all ≤60% (*ca.* 70% for **13**). The activity trend in this case revealed that **13** was the most active and then **4** = **5** >**3** > **1** > **2**.

The dependence of the M_n and molecular weight distribution on the monomer conversion in the reactions catalyzed by **5**/BnOH was also investigated (Fig. 12). For the ROP of ε-CL, the polymer M_n was shown to increase linearly with the conversion, while the M_w/M_n was found to be rather constant at *ca.* 1.14 throughout the reaction (Fig. 12, left). A similar outcome was also observed in the reaction involving δ-VL (Fig. 12, right).

Finally, the kinetic behaviour of complex **5** in the ROP of ε-CL was compared to that of catalysts **12** and **13** both under inert and aerobic conditions (Fig. 13). In the presence of the calix[4]arene-based complexes **13** and **5**, the reaction rate of the polymerization conducted in air was shown to be similar to that of the runs preformed under inert atmosphere. On the contrary, a detrimental effect was observed when the bi-phenolate complex **12** was employed in air compared to the reaction carried out under inert atmosphere.

Silica immobilization of complex 5

Complex **5** was immobilized on pre-treated silica by refluxing in toluene affording structure Si-**5**; the silica was heated at 200 °C under dynamic vacuum for 2 h. X-ray photoelectron spectroscopy (XPS) analysis of the silica surface was performed

Table 7 Comparison between the activities of various Ti-based ROP catalysts

Run	Catalyst	Monomer	M : Ti : BnOH	T (°C)	t (h)	Conv.[a] (%)	$M_{n(corr)}$[b,c]	$M_{n(calc)}$[d]	M_w/M_n[b]
1	**5**	ε-CL	500 : 1 : 1	80	24	>99	8100	28 360	1.40
2	**12**		500 : 1 : 2	80	24	53	6390	15 140	1.24
3	**13**		500 : 1 : 2	80	24	24	2540	6950	1.13
4	**[Ti(Oi-Pr)$_4$]**		500 : 1 : 0	80	24	None	—	—	—
5	**5**	δ-VL	500 : 1 : 1	80	24	81	12 570	40 650	1.37
6	**12**		500 : 1 : 2	80	24	35	7490	8860	1.15
7	**13**		500 : 1 : 2	80	24	33	5700	9500	1.13
8	**[Ti(Oi-Pr)$_4$]**		500 : 1 : 0	80	24	None	—	—	—
9	**5**	*r*-LA	500 : 1 : 1	130	24	97	28 830	69 650	1.94
10	**12**		500 : 1 : 2	130	24	80	8870	28 900	1.61
11	**13**		500 : 1 : 2	130	24	77	10 700	27 830	1.20
12	**[Ti(Oi-Pr)$_4$]**		500 : 1 : 0	130	24	None	—	—	—
13	**5**	ω-PDL	500 : 1 : 2	130	24	53	2835[e]	63 710	nd
14	**12**		500 : 1 : 2	130	24	None	—	—	—
15	**13**		500 : 1 : 1	130	24	12	—	—	—
16	**[Ti(Oi-Pr)$_4$]**		500 : 1 : 0	130	24	None	—	—	—

Reaction conditions: toluene 5 mL, [monomer] = 0.9 M, N_2. [a] Determined by ^{1}H NMR spectroscopy on crude reaction mixture based on ε-CL. [b] From GPC. [c] M_n values were determined by GPC in THF *vs.* PS standards and were corrected with a Mark–Houwink factor (0.56 for PCL and 0.58 for PLA). [d] Calculated from $([M]_0/[OH]_0 \times \text{Conv.} \times M_{w(\text{monomer})} + M_{w(\text{BnOH})})$. [e] Determined by mass spectrometry.

Open Access Article. Published on 27 2020. Downloaded on 10-11-2024 06:39:06.
This article is licensed under a Creative Commons Attribution 3.0 Unported Licence.

Table 8 ROP of ε-CL under solvent-free conditions in the presence of Ti-based catalysts

Run	Catalyst	ε-CL : Ti : BnOH	T (°C)	t (min)	Conv.[a] (%)	$M_{n(corr)}$[b,c]	$M_{n(calc)}$[d]	M_w/M_n[b]
1	**5**	500 : 1 : 2	100	10	50	8140	14 360	1.14
2	**12**	500 : 1 : 2	100	10	None	—	—	—
3	**13**	500 : 1 : 2	100	10	None	—	—	—
4	**[Ti(O^{i}Pr)$_4$]**	500 : 1 : 0	100	10	30	3270	16 530	1.26

Reaction conditions: no solvent, N_2. [a] Determined by ^{1}H NMR spectroscopy on crude reaction mixture based on ε-CL. [b] From GPC. [c] M_n values were determined by GPC in THF *vs.* PS standards and were corrected with a Mark–Houwink factor (0.56). [d] Calculated from ($[M]_0/[OH]_0 \times$ Conv. $\times M_{w(monomer)} + M_{w(BnOH)}$).

Table 9 ROP of ε-CL in air catalyzed by Ti-based complexes **5**, **12** and **13**

Run	Catalyst	ε-CL : Ti : BnOH	*T* (°C)	*t* (h)	Conv.[a] (%)	$M_{n(corr)}$[b,c]	$M_{n(calc)}$[d]	M_w/M_n[b]
1	**5**	500 : 1 : 2	130	1	85	19 130	24 350	1.82
2	**12**	500 : 1 : 2	130	1	40	4810	12 360	1.13
3	**13**	500 : 1 : 2	130	1	>99	11 550	28 360	1.69
4	**5**	500 : 1 : 2	130	24	>99	4580	28 360	2.08
5	**12**	500 : 1 : 2	130	24	>99	5460	28 360	3.12

Reaction conditions: toluene 5 mL, [ε-CL] = 0.9 M, air. [a] Determined by ^{1}H NMR spectroscopy on crude reaction mixture based on ε-CL. [b] From GPC. [c] M_n values were determined by GPC in THF *vs.* PS standards and were corrected with a Mark–Houwink factor (0.56). [d] Calculated from ($[M]_0/[OH]_0 \times$ Conv. $\times M_{w(monomer)} + M_{w(BnOH)}$).

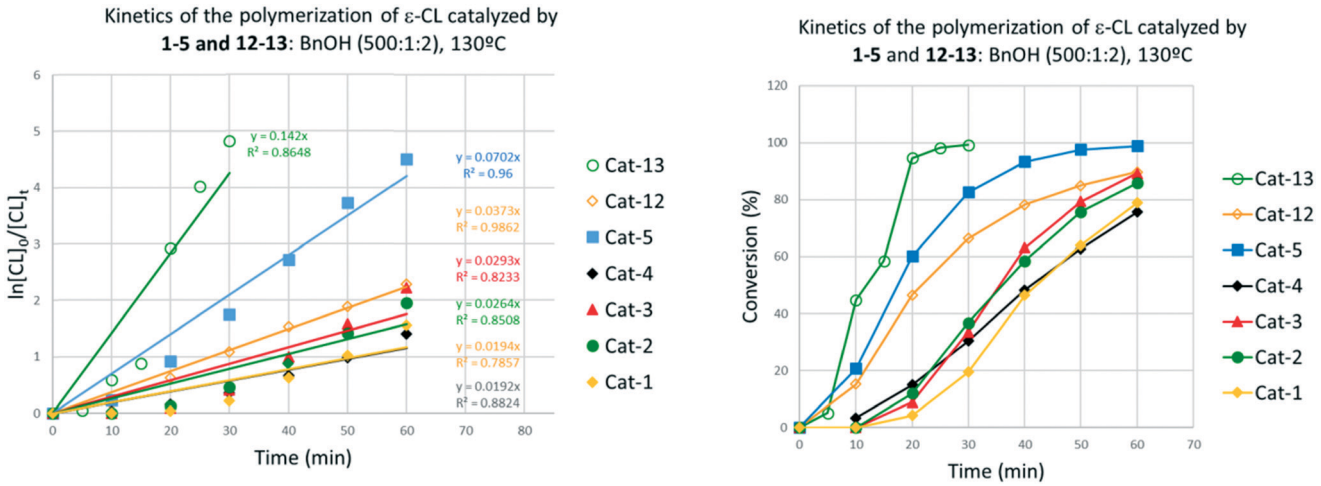

Fig. 10 Left: Plot of ln[CL]$_0$/[CL]*t* *vs.* time using complexes **1**–**5**; right: relationship between conversion and time for the polymerization of ε-CL.

(Fig. 14). The region area ratios of the C-1s to Ti-2p indicated a Ti content of 1.89% with respect to C. This was slightly lower than the calculated value (2.17%) and allegedly due to adventitious carbon bound to the surface. However, this evidence suggested that no decomposition occurred on binding the complex to the surface. Moreover, the Ti-2p peak was consistent with the presence of only one titanium species.

Polymerization of cyclic esters catalyzed by Si-5

The supported version of complex **5** was tested in the ROP of cyclic esters (Table 10). For each run, 50 mg of catalyst were employed. Based on the Ti content found by XPS analysis, the monomer/Ti ratio was found to be 400. Si-**5** proved to be very active in the reaction involving ε-CL. Complete conversion was observed after 24 h at 130 °C both in the presence and in the absence of 1 equiv. of alcohol (runs 1 and 2). Interestingly, higher molecular mass and better control was observed in the experiment conducted in the absence of the co-catalyst. While high conversions were achieved with the homogeneous complex **5** after 1 h (85%, *cf.* Table 1, entry 13), lower activity was observed in the case of its supported version (runs 3 and 4). The catalyst proved to be active also in the ROP of δ-VL and *rac*-LA albeit with moderate activity (runs 5 and 6). While low control was observed for the former, narrow polydispersity was achieved for the latter (2.48 *vs.* 1.15, respectively). Unlike its homogeneous analogues, system Si-**5** was not active in the ROP of the larger monomer ω-pentadecalactone (run 7).

 This journal is © The Royal Society of Chemistry 2020

Open Access Article. Published on 27 2020. Downloaded on 10-11-2024 06:39:06.
This article is licensed under a Creative Commons Attribution 3.0 Unported Licence.

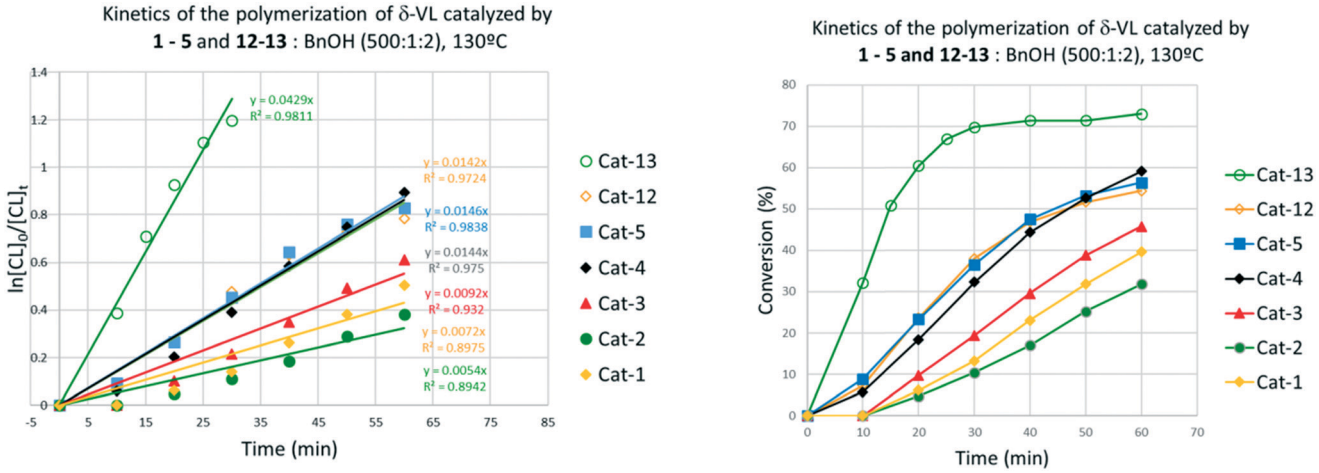

Fig. 11 Left: Plot of $\ln[VL]_0/[VL]t$ *vs.* time using complexes **1**–**5** and **12**–**13**; right: relationship between conversion and time for the polymerization of δ-VL.

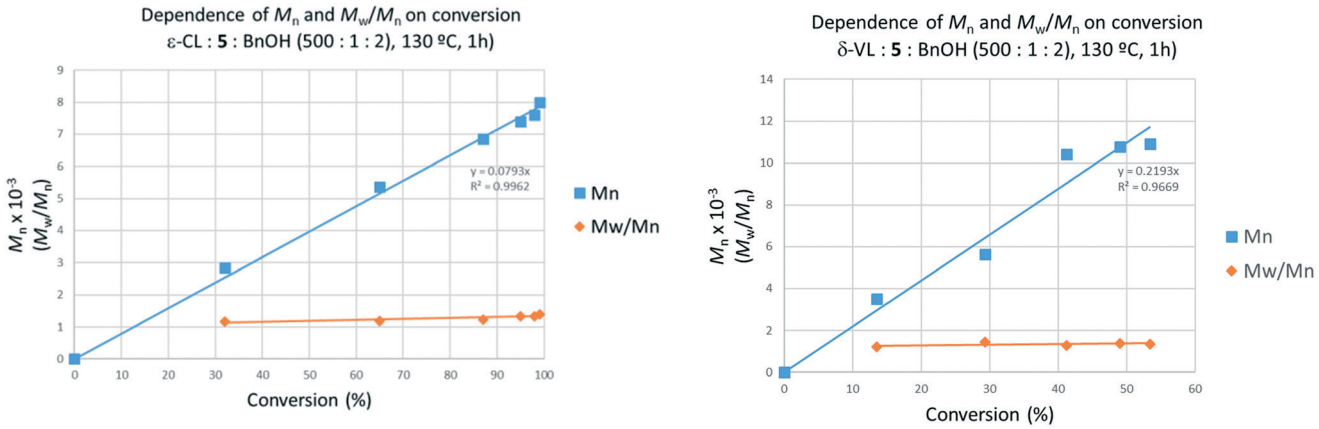

Fig. 12 Dependence of M_n and polydispersity on conversion in the ROP of cyclic esters catalyzed by **5**. Left: ε-CL; right: δ-VL.

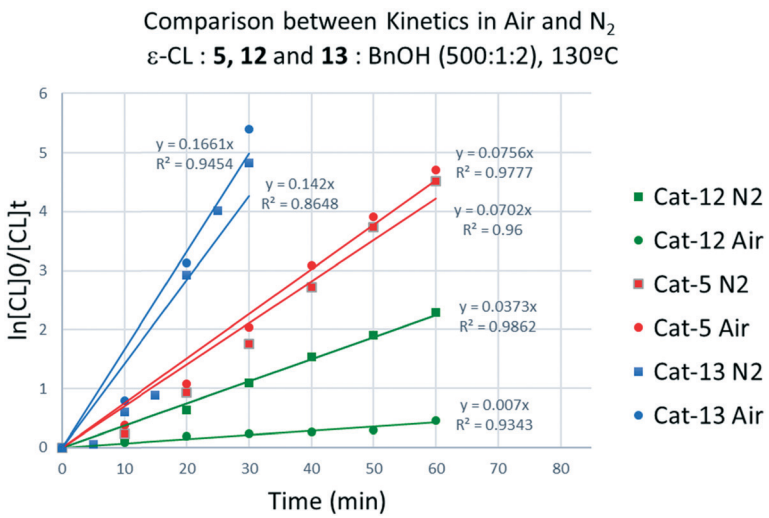

Fig. 13 Comparison between the kinetic behaviour of catalysts **5**, **12** and **13** in the ROP of ε-CL (inert and aerobic conditions).

In conclusion, we have isolated and structurally characterized a number of titanocalix[4]arene complexes which are capable of the ROP of cyclic esters. In particular, we find that a mono-methoxy complex [Ti(NCMe)Cl(L(O)$_3$-

Open Access Article. Published on 27 2020. Downloaded on 10-11-2024 06:39:06.
This article is licensed under a Creative Commons Attribution 3.0 Unported Licence.

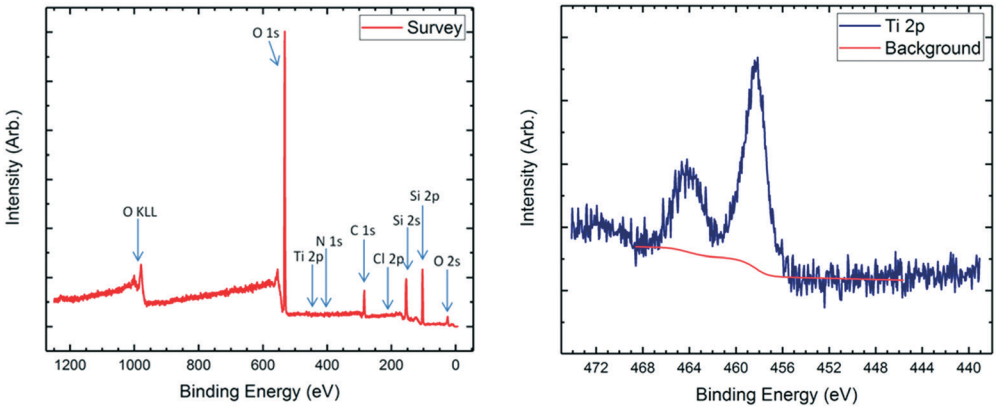

Fig. 14 Left: Full X-ray photoelectron survey spectrum of Si-**5**. Right: Titanium Ti-2p energy window 475–440 eV.

Table 10 Polymerization of cyclic esters catalyzed by Si-supported-**5**

Run	Monomer	Monomer : M : BnOH	T (°C)	t (h)	Conv.[a] (%)	M_n[b,c]	M_w/M_n[b]
1	ε-Caprolactone	400 : 1 : 0	130	24	>99	9750	2.09
2		400 : 1 : 1	130	24	>99	4840	2.77
3		400 : 1 : 0	130	1	35	—	—
4		400 : 1 : 1	130	1	25	—	—
5	δ-Valerolactone	400 : 1 : 0	130	24	61	23 260	2.48
6	*rac*-Lactide	400 : 1 : 0	130	24	78	20 340	1.15
7	ω-pentadecalactone	400 : 1 : 0	130	24	2	—	—

Reaction conditions: ε-CL 4.5 mmol (400 equiv.), supported catalyst 50 mg, toluene 5 mL, 130 °C, 24 h, N_2. [a] Determined by ^{1}H NMR spectroscopy on crude reaction mixture. [b] From GPC. [c] M_n values were determined by GPC in THF *vs.* PS standards and were corrected with a Mark–Houwink factor (M_n,GPC × 0.56 for ε-CL, 0.58 for *r*-LA).

(OR))]·MeCN exhibits superior behavior (K_{obs} 1.3 × 10^{-3} s^{-1} for CL; 2.5 × 10^{-4} s^{-1} for VL) compared with the dialkoxy-type complexes [$TiCl_2L(O)_2(OR)_2$] (R = Me, *n*-Pr and *n*-pentyl) (K_{obs} 6.4 × 10^{-4} s^{-1} for CL; 1.8 × 10^{-4} s^{-1} for VL – complex **3**), which is thought to be due to the lability of the metal-bound acetonitrile under ROP conditions. Importantly, the ROP of both ε-CL and δ-VL can be conducted under air without loss of activity. It also proved possible to ROP the larger cyclic ester ω-PDL with moderate conversation (*ca.* 50%). Complex **5** was able to co-polymerize ε-CL and δ-VL with the same activity, while higher poly-lactide content was observed in the ε-CL/*rac*-LA co-polymerization. We have also investigated the air and moisture stability of some of these titanocalix[4]arenes, and have isolated and structurally characterized bridged OH^-/Cl^- species.

Experimental

General

All manipulations were carried out under an atmosphere of dry nitrogen using conventional Schlenk and cannula techniques or in a conventional nitrogen-filled glove box. Hexane and toluene were refluxed over sodium. Acetonitrile was refluxed over calcium hydride. All solvents were distilled and degassed prior to use. IR spectra (nujol mulls, KBr windows) were recorded on a Nicolet Avatar 360 FT IR spectrometer; ^{1}H NMR spectra were recorded at room temperature on a Varian VXR 400 S spectrometer at 400 MHz or a Gemini 300 NMR spectrometer or a Bruker Advance DPX-300 spectrometer at 300 MHz. The ^{1}H NMR spectra were calibrated against the residual protio impurity of the deuterated solvent. Elemental analyses were performed by the elemental analysis service at the London Metropolitan University and in the Department of Chemistry, the University of Hull. The precursor [$TiCl_4(THF)_2$] was prepared by the literature method.[24] The pro-ligands $L(OH)_2(OR)_2$ were prepared as described previously.[25] Complex **13** was synthesized according to the literature procedures.[8] All other chemicals were purchased from Sigma Aldrich or TCI UK/China.

Synthesis of [$TiCl_2L(O)_2(OR)_2$] (R = Me (1), *n*-Pr (2), *n*-pentyl (3)) and {[$TiL(O)_3(OR)$]$_2$(μ-Cl)$_2$} (R = *n*-decyl (4))

The method employed here was a modification of that reported by Taoufik and Bonnamour,[5] except for R = *n*-decyl, where [$TiCl_4$] was employed. A representative example is [$TiCl_4(THF)_2$] (0.50 g, 1.50 mmol) was added to $L^1H_2Me_2$ (1.00 g, 1.48 mmol) in toluene and stirred at 60 °C for 12 h. On cooling, volatiles were removed, and extraction into MeCN (40 mL) afforded on standing for 24 h at 0 °C the complex as the acetonitrile solvate.

This journal is © The Royal Society of Chemistry 2020

Open Access Article. Published on 27 2020. Downloaded on 10-11-2024 06:39:06.
This article is licensed under a Creative Commons Attribution 3.0 Unported Licence.

For **1** (0.62 g, 53%): $C_{46}H_{58}Cl_2O_4Ti{\cdot}(C_2H_3N)$ requires C 69.06, H 7.37, N 1.68% found C 68.91, H 7.52, N 1.41%. IR: 2246w, 1596w, 1414w, 1363m, 1306m, 1261s, 1207s, 1159 m, 1088s, 1019s, 994s, 948s, 939m, 918w, 869m, 796s, 747w, 706w, 680w. ^{1}H NMR (C_6D_6, 298 K) δ: 7.14 (s, 4H, aryl*H*), 6.81 (s, 4H, aryl*H*), 4.61 (d, 4H, J = 13 Hz, *endo*-CH_2), 4.18 (s, 6H, OCH_3) 3.18 (d, 4H, J = 13 Hz, *exo*-CH_2), 1.36 (s, 18H, C(CH_3)$_3$), 0.67 (s, 18H, C(CH_3)$_3$), 0.29 (s, 3H, CH_3CN).

For **2**, yield 0.71 g, 56%. $C_{50}H_{66}Cl_2O_4Ti{\cdot}2(C_2H_3N)$ requires C 69.60, H 7.79, 3.01 N% found C 68.89, H 8.32, N 2.83%. IR: 2245w, 1595w, 1413w, 1377m, 1309m, 1260s, 1200s, 1158w, 1117m, 1086s, 1024s, 960m, 937w, 874m, 858m, 795s, 744w, 702w, 677w. ^{1}H NMR ($CDCl_3$, 298 K) δ: 7.08 (s, 4H, aryl*H*), 6.99 (s, 4H, aryl*H*), 4.91 (m, 4H, OCH_2), 4.54 (d, 4H, J = 13 Hz, *endo*-CH_2), 3.36 (d, 4H, J = 13 Hz, *exo*-CH_2), 2.04 (m, 4H, OCH$_2$CH_2), 1.9 (s, 6H, CH_3CN), 1.33 (s, 18H, C(CH_3)$_3$), 1.15 (s, 18H, C(CH_3)$_3$), 0.85 (t, 6H, J = 7.6 Hz,CH_3CH$_2$).

For **3**: yield 0.78 g, 57%. $C_{54}H_{74}Cl_2O_4Ti{\cdot}1.5(C_2H_3N)$ requires C 70.76, H 8.11, N 2.17% found C 70.47, H 8.39, N 2.30%. IR: 1601w, 1413w, 1377m, 1306m, 1260s, 1209m, 1158w, 1087s, 1020s, 937m, 873m, 863m, 795s, 746w, 677w. ^{1}H NMR ($CDCl_3$, 298 K) δ: ^{1}H NMR ($CDCl_3$, 298 K) δ: 7.09 (s, 4H, aryl*H*), 7.00 (s, 4H, aryl*H*), 4.91 (m, 4H, OCH_2), 4.54 (d, 4H, J = 13 Hz, *endo*-CH_2), 3.36 (d, 4H, J = 13 Hz, *exo*-CH_2), 2.02 (m, 4H, OCH$_2$CH_2), 1.74 (s, 4.5H, CH_3CN), 1.38 (s, 18H, C(CH_3)$_3$ overlapping with m, 4H, OCH$_2$CH$_2$CH_2CH$_3$), 1.16 (s, 18H, C(CH_3)$_3$ overlapping with m, 4H, OCH$_2$CH$_2$CH_2CH$_3$), 0.84 (t, 6H, J = 6.4 Hz,CH_3CH$_2$).

For **4**: yield 0.88 g, 66%. $C_{108}H_{146}Cl_2O_8Ti_2(C_2H_3N)$ requires C 74.22, H 8.44, N 0.80%. Found C 74.70, H 8.92, N 0.67%. IR: 2249w, 1601w, 1580w, 1415w, 1393m, 1377s, 1363s, 1302m, 1256m, 1205s, 1172w, 1122m, 1113m, 1094m, 1022w, 974w, 944s, 925m, 876s, 864m, 831m, 798s, 761m, 723w, 678w. ^{1}H NMR ($CDCl_3$) δ: 7.08 (m, 4H, aryl*H*), 7.03 (s, 2H, aryl*H*), 7.02 (s, 2H, aryl*H*), 4.91 (d, 2H, J = 12 Hz, *endo*-CH_2), 4.23 (d, 4H, J = 12 Hz, *endo*-CH_2), 4.38 (m, 4H, OCH_2), 3.20 (m, 4H, *exo*-CH$_2$), 2.05 (s, 1.5H, 0.5MeCN), 1.85 (bm, 4H, CH_2), 1.33 (s, 18H C(CH_3)$_3$), 1.27–1.16 (overlapping m, 28H, CH_2), 0.74 (s, 9H C(CH_3)$_3$), 0.88 (m, 6H, CH_3), 0.66 (s, 9H C(CH_3)$_3$), 0.46 (s, 3H, *Me*CN).

Synthesis of [Ti(NCMe)Cl(LMe)]·MeCN·(5·MeCN)

As for **1**, but the system was refluxed for 60 h, and then following removal of volatiles, the residue was stirred in MeCN (40 mL) for 24 h. Filtration, concentrated to half volume, and prolonged standing at 0 °C afforded orange/red crystals of 7·MeCN. Yield 0.82 g, 74%. $C_{49}H_{61}N_2ClO_4Ti$ requires C 71.30, H 7.45, N 3.39%. Found C 71.00, H 7.68, N 3.65%. IR: 2306w, 2286w, 2245w, 1599w, 1413m, 1364s, 1307s, 1276m, 1256s, 1203s, 1167m, 1118m, 1095m, 1005s, 946m, 934s, 917m, 901w, 874s, 845m, 824m, 811w, 799s, 780m, 756m, 722m, 680m. MS (positive nanoelectrospray): 754.3 (MH^+ –OMe). ^{1}H NMR (C_6D_6) δ: 7.08 (m, 4H, aryl*H*), 7.03 (s, 2H, aryl*H*), 7.02 (s, 2H, aryl*H*), 4.77 (d, 2H, J = 12 Hz, *endo*-CH$_2$), 4.37 (d, 2H, J = 12 Hz, *endo*-CH$_2$), 4.23 (s, 3H, OCH_3), 3.34 (overlapping d, J = 12 Hz, 4H, *exo*-CH$_2$), 1.85 (s, 3H, *Me*CN), 1.25 (s, 18H C(CH_3)$_3$), 1.19 (s, 9H C(CH_3)$_3$), 1.16 (s, 9H C(CH_3)$_3$).

Synthesis of {[TiL(O)$_3$(O*n*-Pr)]$_2$(μ-Cl)(μ-OH)}·7MeCN (6·7MeCN)

As for **5**, but using L(O)$_2$(*n*-PrO)$_2$ (0.50 g, 0.68 mmol) and TiCl$_4$·(THF)$_2$ (0.23 g, 0.68 mmol) affording **6** as orange/red prisms. Yield: 0.53 g, 40%. $C_{99}H_{125}N_2ClO_9Ti_2$ (sample dried *in vacuo* for 12 h, –5MeCN) requires C 73.27, H 7.84, N 1.74%. Found C 74.05, H 8.78, N 1.33%. IR: 3730w, 3698w, 3589w, 3335w, 3190w, 2730w, 1750w, 1645w, 1597w, 1410m, 1380m, 1305m, 1257s, 1200s, 1177w, 1093s, 1017s, 940m, 925m, 866w, 800s, 760w, 720w, 675w, 660w. ^{1}H NMR ($CDCl_3$) δ: 7.06–6.97 (m, 16H, Aryl*H*), 4.80 (d, 2H, J = 13, *endo*-CH_2), 4.54–4.44 (m, 8H, *endo*-CH_2 overlapped with OCH_2CH$_2$CH$_3$), 3.30 (m, 8H, overlapping *exo*-CH_2), 1.92 (m, 4H, OCH$_2$CH_2CH$_3$), 1.64 (s, 6H, 2CH_3CN), 1.26–0.97 (m, 54H, C(CH_3)$_3$ overlapping with OCH$_2$CH$_2$CH_3), OH signal not detected.

Synthesis of {[TiL(O)$_3$(O*n*-pentyl)]$_2$(μ-Cl)(μ-OH)}·7.5MeCN (7·7.5MeCN)

As for **5**, but using L(O)$_2$(*n*-pentylO)$_2$ (1.00 g, 1.27 mmol) and TiCl$_4$ (1.29 mL, 1 M in CH_2Cl_2, 1.29 mmol) affording **7** as orange/red prisms. Yield: 0.89 g, 74%. The sample was dried *in vacuo* for 12 h (–7.5 CH_3CN). $C_{98}H_{127}ClO_9Ti_2$·requires C 74.49, H 8.09. Found C 73.76, H 8.57. IR: 2955w, 2920s, 2850m, 2724w, 1460s, 1378s, 1300w, 1260m, 1210w, 1155w, 1090m, 1020m, 970w, 940w, 920w, 890w, 875w, 800m, 720m, 560w. ^{1}H NMR ($CDCl_3$) δ: 7.00–6.76 (m, 16 H, Aryl*H*), 5.10 (t, 4 H, J = 10 Hz, OCH_2CH$_2$CH$_2$CH$_2$CH$_3$), 4.97 (d, 8 H, J = 13 Hz, *endo*-CH_2), 3.27 (d, 8 H, J = 13, *exo*-CH_2), 2.80 (m, 4 H, OCH$_2$CH_2CH$_2$CH$_2$CH$_3$), 1.33 (s, 36 H, (C(CH_3)$_3$)), 0.90 (m, 8 H, OCH$_2$CH$_2$CH_2CH_2CH$_3$), 0.83 (s, 36 H, (C(CH_3)$_3$)), 0.60 (6 H, t, J = 9, OCH$_2$CH$_2$CH$_2$CH$_2$CH_3). OH signal not detected.

Synthesis of [Ti(NCMe)(μ$_3$-O)L(O)$_4$TiCl(O(CH$_2$)$_4$Cl)]$_2$–2[TiCl(NCMe)(L(O)$_3$(O*n*-Pr))]·11MeCN (8·11MeCN)

L(O)$_2$(*n*-PrO)$_2$ (1.00 g, 1.36 mmol) and TiCl$_4$(THF)$_2$ (0.46 g, 1.38 mmol) in toluene (30 mL) was refluxed for 60 h. On cooling, the volatiles were removed *in vacuo*, and the residue was extracted into MeCN (30 mL). On standing at 0 °C, large red prisms formed. Yield 0.75 g, 56%. $C_{198}H_{250}N_4Cl_6O_{20}Ti_6$ (sample dried *in vacuo* for 12 h) requires C 67.82, H 7.19, N 1.60%. Found C 68.81, H 8.32, N 2.83%.[26] IR: 3650w, 3184w, 2728w, 1771w, 1603w, 1580w, 1417m, 1392s, 1314s, 1279s, 1262s, 1209s, 1115s, 1096s, 1029s, 988s, 939m, 921s, 874s, 862s, 823s, 796s, 754m, 679m. ^{1}H NMR ($CDCl_3$) δ: 7.19–6.95 (m, 16H aryl*H* dimer overlapped with 8H aryl*H* mono-Cl-complex), 4.81 (d, 4H, J = 13 Hz, *endo*-CH_2 dimer), 4.56 (d, 4H, J = 13 Hz, *endo*-CH_2 dimer), 4.45 (d, 2H, *endo*-CH_2 mono-Cl complex) partially overlapped with 4.33 (m, 2H, OCH_2CH$_2$CH$_3$ mono-Cl complex), 3.70 (m, 4H, ClCH_2CH$_2$CH$_2$-CH$_2$O–), 3.58 (m, 4H, ClCH$_2$CH$_2$CH$_2$CH_2O–), 3.29 (m, 4H *exo*-

Open Access Article. Published on 27 2020. Downloaded on 10-11-2024 06:39:06.
This article is licensed under a Creative Commons Attribution 3.0 Unported Licence.

CH_2 dimer overlapped with 2H *exo*-CH_2 mono-Cl complex), 3.05 (d, 2H, 13 Hz, *exo*-CH_2 mono-Cl complex), 2.24 (m, 4H, $ClCH_2CH_2CH_2CH_2O$–), 1.98 (m, 4H, $ClCH_2CH_2CH_2CH_2O$–) partially overlapped with 1.86 (m, 2H, $OCH_2CH_2CH_3$ mono-Cl complex), 1.56–1.23 (m, 72H $C(CH_3)_3$ dimer overlapped with 36H, $C(CH_3)_3$ mono-Cl complex), 0.99 (m, 3H, $OCH_2CH_2CH_3$ mono-Cl complex).

Synthesis of {[TiL(*n*-pentyl)]$_2$(μ-Cl)(μ-OH)}·9MeCN (9·9MeCN)

Complex **3** (1.00 g, 1.10 mmol) in toluene (30 mL) was stirred under air for 1 h, the volatiles were removed *in vacuo* and the residue was extracted into warm (brief heating with a hot-gun) acetonitrile (30 mL). The solution was left to stand (3 to 4 days) affording on standing orange/red crystals of **9**. Yield: 0.73 g, 68%. The sample was dried *in vacuo* for 12 h (−9 MeCN). $C_{98}H_{127}ClO_9Ti_2$ requires C 74.49, H 8.10. Found C 73.29, H 8.48. IR: 298w, 2919s, 2852m, 2726w, 1463s, 1380s, 1298w, 1258m, 1207w, 1157w, 1088m, 1015m, 967w, 943w, 925w, 893w, 878w, 803m, 725m, 561w. ^{1}H NMR ($CDCl_3$) δ: 7.10–6.80 (m, 16 H, Aryl*H*), 5.13 (t, 4 H, J = 9 Hz, $OCH_2CH_2CH_2CH_2CH_3$), 4.94 (d, 8 H, J = 12 Hz, *endo*-CH_2), 3.22 (d, 8 H, J = 12, *exo*-CH_2), 2.74 (m, 4 H, $OCH_2CH_2CH_2CH_2CH_3$), 1.36 (s, 36 H, $C(CH_3)_3$)), 0.87 (m, 8 H, $OCH_2CH_2CH_2CH_2CH_3$), 0.80 (s, 36 H, $C(CH_3)_3$)), 0.62 (6 H, t, J = 9, $OCH_2CH_2CH_2CH_2CH_3$). OH signal not detected.

{[TiL(*n*-decyl)]$_2$(μ-Cl)(μ-OH)}·8.5MeCN (10·8.5MeCN)

As for **9**, but using L(*n*-decyl)$_2$ (1.00 g, 1.08 mmol) and $TiCl_4$ (0.12 mL, 1.09 mmol) affording **10** as orange blocks. Yield: 0.54 g, 48%. $C_{108}H_{147}ClO_9Ti_2$·8.5MeCN. Sample dried *in vacuo* for 12 h (−7.5 MeCN) requires C 74.87, H 8.74, N 0.79%. Found C 74.70, H 8.92, N 0.67%. IR: 3728w, 3702w, 3596w, 3332w,3187w, 2727w, 1748w, 1647w, 1601w, 1416m, 1377m, 1301m, 1260s, 1205s, 1173w, 1095s, 1020s, 938m, 921m, 861w, 796s, 757w, 723w, 678w, 661w. ^{1}H NMR ($CDCl_3$) δ: 7.05 (m, 4H, Aryl*H*), 6.99 (s, 4H, Aryl*H*), 4.80 (d, 2H, J = 12, *endo*-CH_2), 4.50–4.10 (m, 4H, *endo*-CH_2 overlapped with OCH_2CH_2–), 4.23 (overlapping d, 6H, *exo*-CH_2), 1.87 (s, 3H, *Me*CN), 1.25–1.16 (m, 52H, $C(CH_3)_3$ overlapping with CH_2-decyl), 0.89 (m, 6H, CH_3). OH signal not detected.

[Ti$_2$(μ-OH)(μ-Cl)(L*n*-pentyl)]$_2$[L(*n*-pentyl)$_2$]·2.85(C_2H_3N)·0.43(H_2O) (11·2.85(C_2H_3N)·0.43(H_2O))

To **3** (1.00 g, 1.10 mmol) in toluene (30 mL) was added H_2O (0.01 mL, 0.56 mmol) and the system was refluxed for 12 h. Volatiles were removed *in vacuo*, and the residue was extracted into warm MeCN (30 mL). On prolonged standing at ambient temperature, orange plate-like crystals of **11** formed. Yield: 0.79 g, 69%. The sample was dried under reduced pressure for 12 h (−2.85 CH_3CN, −0.43 H_2O). $C_{112.5}H_{165}ClO_{11}Ti_2$ requires C 74.05, H 9.11%. Found C 73.27, H 8.73, N <0.1%. IR: 3647w, 3344w, 3228w, 2726w, 2671w, 2379w, 2289w, 2249w, 1748w, 1600w, 1414s, 1393s, 1377s, 1363s, 1302m, 1281s, 1260s, 1207s, 1115m, 1095m, 1039m, 1019m, 974m, 938m, 921m, 874s, 827s, 810s, 798s, 768m, 758m, 723m, 679m. ^{1}H NMR (C_6D_6) δ = 10.28 (s, 2H, ArylO*H*), 7.17 (m, 2H, Aryl*H*), 7.02 (m, 2H, Aryl*H*), 6.94 (m, 8H, Aryl*H*) 6.74 (m, 8H, Aryl*H*), 5.33 (m, 4H, OCH_2CH_2–), 4.93 (d, 4H J = 12 Hz, *endo*-CH_2), 4.82 (d, 4H J = 12 Hz, *endo*-CH_2) 4.47 (d, 4H J = 12 Hz, *endo*-CH_2) 4.32 (m, 6H, *exo*-CH_2 overlapped with $OCH_2CH_2CH_2CH_2CH_3$), 3.22 (m, 8H, *exo*-CH_2 *overlapped with* $OCH_2CH_2CH_2CH_2CH_3$), 2.05 (s, 3H, *Me*CH), 3.19–3.16 (m, 16 H, $OCH_2CH_2CH_2CH_2CH_3$), 1.32 (s, 18 H, $(C(CH_3)_3)$), 1.30 (s, 18H, $C(CH_3)_3$), 1.06 (s, 18 H, $C(CH_3)_3$), 1.05 (s, 18 H, $C(CH_3)_3$), 1.01 (8 H, m, $OCH_2CH_2CH_2CH_2CH_3$), 0.45 (m, 12 H, –$OCH_2CH_2CH_2CH_2CH_3$). OH signal not detected.

[Ti(Cl)$_2$(6,6′-(ethane-1,1-diyl)bis(2,4-di-*tert*-butylphenolate))] (12)

To a suspension of 2,2′-CH_3CH[4,6-(*t*-Bu)$_2C_6H_2O$]$_2$ (2.0 g, 5.9 mmol) in dry hexane (30 mL), [$TiCl_4$] (0.65 mL, 5.9 mmol, 1 equiv.) was added dropwise. The mixture was stirred at room temperature for 16 h affording a deep-red solid which was collected by filtration and dried under reduced pressure at room temperature for 4 h. Yield 2.0 g (3.6 mmol, 61%). Requires C 64.87, H 7.98%. Found C 64.72, H 8.25%. IR: 1220 cm^{-1} m, 1200m, 1105w, 922m, 628w, 475m, 437w, 410m, 365w. ^{1}H NMR (C_6D_6) δ 7.53 (d, J = 2.3 Hz, 2H, Ar*H*), 7.23 (d, J = 2.3 Hz, 2H, Ar*H*), 4.71 (q, J = 6.7 Hz, 1H, $CH(CH_3)$), 1.37–1.61 (s, 18H, $C(CH_3)_3$ overlapping with d, 3H, CH_3), 1.23 (s, 18H, $C(CH_3)_3$).

Preparation of silica supported complex (Si-5)

SiO_2 pretreatment: silica gel (60 Å, mesh 35–70 μm, 5.0 g) was heated at 200 °C under vacuum for 2 h.

Immobilization of the complex: a solution of **5** in toluene (0.07 g in 10 mL) was added to a suspension of the pre-treated silica in toluene (500 mg in 10 mL). The mixture was stirred at reflux for 16 h and then allowed to cool down to room temperature. The mixture was filtered, and the solid residue was washed with warm toluene (2 × 10 mL) and dried under reduced pressure at room temperature for 2 h affording a yellow fine powder (0.46 g).

Ring open polymerization (ROP) procedures

ε-Caprolactone (ε-CL): typical polymerization procedures are as follows. A toluene solution of **1** (0.010 mmol, in 1.0 mL toluene) was added into a Schlenk tube in the glove-box at room temperature. The solution was stirred for 2 min, and then ε-caprolactone (2.5 mmol) along with 1.5 mL toluene was added to the solution. The reaction mixture was then placed into an oil bath pre-heated to the required temperature, and the solution was stirred for the prescribed time. The polymerization mixture was then quenched by addition of an excess of glacial acetic acid (0.2 mL) into the solution, and the resultant solution was then poured into methanol (200 mL). The resultant polymer was then collected on filter paper and was dried *in vacuo*.

This journal is © The Royal Society of Chemistry 2020

Open Access Article. Published on 27 2020. Downloaded on 10-11-2024 06:39:06.
This article is licensed under a Creative Commons Attribution 3.0 Unported Licence.

Table 11 Crystallographic data

Compound	**2**·2MeCN	**4**·6MeCN	**5**·MeCN	**6**·7MeCN	**7**·7.5MeCN	**8**·11MeCN	**9**·9MeCN	**10**·8.5MeCN	**11**·2.85MeCN ·0.43(H_2O)	**12**
Formula	$C_{50}H_{66}Cl_2O_4Ti$ ·2(C_2H_3N)	$C_{108}H_{146}Cl_2O_8Ti_2$ ·6(C_2H_3N)	$C_{47}H_{58}ClNO_4Ti$ ·(C_2H_3N)	$C_{94}H_{119}ClO_9Ti_2$ ·7(C_2H_3N)	$C_{98}H_{127}ClO_9Ti_2$ ·7.5(C_2H_3N)	$C_{198}H_{250}Cl_6N_4O_{20}Ti_6$ ·11(C_2H_3N)	$C_{98}H_{127}ClO_9Ti_2$ ·9(C_2H_3N)	$C_{108}H_{147}ClO_9Ti_2$ ·8.5(C_2H_3N)	$C_{125}H_{165}ClO_{11}Ti_2$ ·2.85(C_2H_3N) ·0.43H_2O	$C_{30}H_{44}Cl_2O_2Ti$
Formula weight	931.93	1985.26	825.34	1811.51	1888.14	3957.70	1949.72	2069.45	2099.63	555.45
Crystal system	Monoclinic	Triclinic	Triclinic	Triclinic	Monoclinic	Triclinic	Monoclinic	Triclinic	Triclinic	Monoclinic
Space group	*C*2/*c*	$P\bar{1}$	$P\bar{1}$	$P\bar{1}$	$P2_1/n$	$P\bar{1}$	$P2_1/n$	$P\bar{1}$	$P\bar{1}$	$P2_1$
a (Å)	43.9803(4)	12.5697(2)	12.14575(13)	13.9465(2)	26.6007(4)	17.6510(2)	26.5998(4)	17.4371(7)	16.3253(4)	11.0509(2)
b (Å)	12.41683(17)	18.1183(4)	18.0271(2)	17.4744(3)	13.18235(14)	18.2749(2)	13.18144(15)	17.7765(4)	17.3213(3)	9.69430(18)
c (Å)	19.4608(2)	27.5282(3)	21.0909(2)	23.5392(2)	32.7812(5)	19.8507(2)	32.7719(4)	21.1345(4)	23.5069(3)	14.8668(3)
α (°)	90	104.5590(15)	95.2564(9)	85.6028(11)	90	67.4531(11)	90	100.630(2)	102.481(2)	
β (°)	94.9954(10)	98.7810(13)	105.3553(9)	74.2347(12)	104.6220(17)	68.6833(11)	104.6288(14)	93.526(3)	91.495(2)	108.131(2)
γ (°)	90	102.0930(18)	90.2869(9)	74.5316(14)	90	73.3966(12)	90	104.426(3)	101.593(2)	
V (Å^3)	10 587.1(2)	5792.03(18)	4432.27(8)	5320.83(14)	11 122.7(3)	5428.94(12)	11 118.1(3)	6195.8(3)	6340.9(2)	1513.61(5)
Z	8	2	4	2	4	1	4	2	2	2
Temperature (K)	100(2)	100(2)	100(2)	100(2)	100(2)	100(2)	100(2)	100(2)	100(2)	100(2)
Wavelength (Å)	1.54178	1.54178	1.54178	1.54178	0.71073	0.71075	0.71073	1.54178	0.71073	0.71073
Calculated density (g cm^{-3})	1.169	1.138	1.237	1.131	1.128	1.211	1.165	1.109	1.100	1.219
Absorption coefficient (mm^{-1})	2.63	2.03	2.54	1.95	0.22	0.35	0.23	1.73	0.20	0.48
Transmission factors (min./max.)	0.434, 1.000	0.788, 1.000	0.929, 1.000	0.822, 1.000	0.574, 1.000	0.832, 1.000	0.857, 1.000	0.720, 1.000	0.624, 1.000	0.432, 1.000
Crystal size (mm^3)	0.20 × 0.15 × 0.03	0.21 × 0.13 × 0.02	0.27 × 0.24 × 0.13	0.13 × 0.05 × 0.04	0.90 × 0.13 × 0.02	0.22 × 0.14 × 0.08	0.18 × 0.09 × 0.05	0.15 × 0.05 × 0.03	0.18 × 0.12 × 0.02	0.18 × 0.10 × 0.04
θ(max) (°)	68.2	68.3	68.3	70.1	27.5	28.7	27.5	66.6	27.5	27.5
Reflections measured	49 433	105 088	68 296	98 483	167 629	271 747	133 050	103 194	152 246	34 809
Unique reflections	9646	21 053	31 744	19 826	25 491	28 021	25 475	21 695	29 067	6818
R_{int}	0.043	0.070	0.054	0.055	0.052	0.029	0.046	0.131	0.093	0.023
Reflections with $F^2 > 2\sigma(F^2)$	8677	16 916	29 425	18 665	20 319	24 734	20 200	13 736	17 105	6713
Number of parameters	609	1279	1058	1229	1323	1327	1241	1474	1504	329
R_1 [$F^2 > 2\sigma(F^2)$]	0.041	0.093	0.039	0.094	0.075	0.074	0.065	0.099	0.072	0.029
wR_2 (all data)	0.118	0.260	0.111	0.265	0.204	0.231	0.168	0.293	0.208	0.077
GOOF, *S*	1.07	1.07	1.07	1.09	1.11	1.04	1.09	1.02	1.02	1.07
Largest difference peak and hole (e Å^{-3})	0.64 and −0.42	1.58 and −0.44	0.52 and −0.51	1.07 and −0.46	1.40 and −0.64	2.77 and −2.46	1.00 and −0.71	1.10 and −0.55	1.26 and −0.64	0.28 and −0.40

Open Access Article. Published on 27 2020. Downloaded on 10-11-2024 06:39:06.
This article is licensed under a Creative Commons Attribution 3.0 Unported Licence.

Kinetic studies

The polymerizations were carried out at 130 °C under N_2 atmosphere. The molar ratio of monomer to catalyst to initiator was fixed at 500 : 1 : 2. At appropriate time intervals (10 minutes), 0.5 μL aliquots were removed and quenched with methanol. The solvent was removed *in vacuo* and the percent conversion was determined by ^{1}H NMR spectroscopy in $CDCl_3$.

X-ray photoelectron spectroscopy

A small amount (~1 mg) of powdered sample was pressed onto adhesive carbon tape. High resolution XPS core level measurements were performed with a Specs NAP-XPS (operating under UHV conditions), equipped with a SPECS Phoibos 150 NAP hemispherical analyser. XPS experiments were carried out using a high intensity monochromated Al-Kα source (1486.6 eV) operated at 14.5 kV and 25 mA. Detailed spectra were recorded using a pass energy of 30 eV. The energy scale of the spectrometer was calibrated to the C-1s at 284.8 eV.

Crystal structure determinations

Diffraction data for all crystal structures were collected at low temperature on modern diffractometers equipped with hybrid pixel array detectors and rotating anode X-ray sources.[27] Full details are given in Table 11, in the ESI,† and in the deposited cif files. Data were corrected for absorption and Lp effects.[27] The structures were solved using a dual-space, charge-flipping algorithm and refined on F^2.[28,29] In common with many calixarene crystal structures there are were often some difficulties to overcome during the refinement. Some ^{t}Bu groups needed to be modelled with the methyl groups or the whole moiety split over two sets of positions. MeCNs of crystallization were often disordered and needed to be modelled with split positions, or as diffuse electron density *via* the Platon Squeeze procedure.[30] The number of MeCN molecules of crystallization should only be taken as approximate. Where disorder has been modelled, restraints were applied to anisotropic displacement parameters and the geometry of the affected and immediately adjacent atoms. Hydrogen atoms were placed in geometrically determined positions, except for those on hetero atoms in structures with good data, where coordinates were refined. Exact details of the disorder modelling, *etc.* are given in the ESI† for each individual structure.

CCDC 1954689–97 and 1969053 contain the crystal data for structures **9·9MeCN**, **10·8.5MeCN**, **11·2.85MeCN·0.43H$_2$O**, **2·2MeCN**, **4·6MeCN**, **5·MeCN**, **6·7MeCN**, **7·7.5MeCN**, **8·11MeCN** and **12**, respectively.

Conflicts of interest

There are no conflicts of interest.

Acknowledgements

CR thanks the Shaanxi Province for the 100 Talents Award. We also thank the EPSRC National Crystallography Service at Southampton (UK), the EPSRC Mass Spectrometry Service, Swansea (UK) and the EPSRC for an Overseas Travel Grant (EP/R023816/1) and for the UKRI Creative Circular Plastic grant (EP/S025537/1).

References

1 (*a*) D. H. Homden and C. Redshaw, *Chem. Rev.*, 2008, **108**, 5086–5130; (*b*) Coordination Chemistry and Applications of Phenolic Calixarene–metal Complexes, Y. Li, K.-Q. Zhao, C. Redshaw, B. A. M. Ortega, A. Y. Nuñez and T. A. Hanna in *Patai's Chemistry of Functional Groups*, Wiley, 2014.

2 For early examples see (*a*) M. M. Olmstead, G. Sigel, H. Hope, X. Xu and P. P. Power, *J. Am. Chem. Soc.*, 1985, **107**, 8087–8091; (*b*) A. Zanotti-Gerosa, E. Solari, L. Giannini, C. Floriani, N. Re, A. Chiesi-Villa and C. Rizzoli, *Inorg. Chimica Acta*, 1998, **270**, 298–311; (*c*) W. Clegg, M. R. J. Elsegood, V. C. Gibson and C. Redshaw, *J. Chem. Soc., Dalton Trans.*, 1998, 3037–3039; (*d*) U. Radius, *Inorg. Chem.*, 2001, **40**, 6637–6642; (*e*) F. A. Cotton, E. V. Dikarev, C. A. Murillo and M. A. Petrukhina, *Inorg. Chim. Acta*, 2002, **332**, 41–46.

3 M. Frediani, D. Sémeril, A. Comucci, L. Bettucci, P. Frediani, L. Rosi, D. Matt, L. Toupet and W. Kaminsky, *Macromol. Chem. Phys.*, 2007, **208**, 938–945.

4 C. Capacchione, P. Neri and A. Proto, *Inorg. Chem. Commun.*, 2003, **6**, 339–342.

5 J. Espinas, U. Darbost, J. Pelletier, E. Jeanneau, C. Duchamp, F. Bayard, O. Boyron, J.-P. Broyer, J. Thivolle-Cazat, J.-M. Basset, M. Taoufik and I. Bonnamour, *Eur. J. Inorg. Chem.*, 2010, 1349–1359.

6 (*a*) Y. Li, Y. S. Zheng and G. H. Xie, *Acta Polym. Sin.*, 1998, 101–103; (*b*) Y. Chen, Y. Zhang, Z. Shen and W. Sun, *Acta Polym. Sin.*, 2000, **2**, 239–241; (*c*) A. Diaz-Barrios, J. Liscano, M. Trujillo, G. Agrifoglio and J. O. Matos, Assignee: Intevep S.A., *U.S. Pat.* 5767034, 1998; (*d*) J. O. Matos, A. Diaz-Barrios, J. Liscano, M. Trujillo and G. Agrifoglio, Assignee: Intevep. S.A, *European Pat.* EP1125951, 2001.

7 (*a*) J. M. Notestein, E. Iglesia and A. Katz, *J. Am. Chem. Soc.*, 2004, **126**, 16478–16486; (*b*) J. M. Notestein, L. R. Andrini, V. I. Kalchenko, F. G. Requejo, A. Katz and E. Iglesia, *J. Am. Chem. Soc.*, 2007, **129**, 1122–1131; (*c*) J. M. Notestein, L. R. Andrini, F. G. Requejo, A. Katz and E. Iglesia, *J. Am. Chem. Soc.*, 2007, **129**, 15585–15595; (*d*) Y. Guo, A. Solovyov, N. A. Grosso-Giordano, S.-J. Hwang and A. Katz, *ACS Catal.*, 2016, **6**, 7760–7768.

8 M. Frediani, D. Sémeril, A. Marrioti, L. Rosi, P. Frediani, L. Rosi, D. Matt and L. Toupet, *Macromol. Rapid Commun.*, 2008, **29**, 1554–1560.

9 M. Frediani, D. Sémeril, D. Matt, L. Rosi, P. Frediani, F. Rizzolo and A. M. Papini, *Int. J. Polym. Sci.*, 2010, 490724.

10 J. D. Ryan, K. J. Gagnon, S. J. Teat and R. D. McIntosh, *Chem. Commun.*, 2016, **52**, 9071–9073.

This journal is © The Royal Society of Chemistry 2020

Open Access Article. Published on 27 2020. Downloaded on 10-11-2024 06:39:06.
This article is licensed under a Creative Commons Attribution 3.0 Unported Licence.

11 Y. Li, K.-Q. Zhao, C. Feng, M. R. J. Elsegood, T. J. Prior, X. Sun and C. Redshaw, *Dalton Trans.*, 2014, **43**, 13612–13619.
12 Z. Sun, Y. Zhao, T. J. Prior, M. R. J. Elsegood, K. Wang, T. Xing and C. Redshaw, *Dalton Trans.*, 2019, **48**, 1454–1466.
13 A. Zanotti-Gerosa, E. Solari, L. Giannini, C. Floriani, N. Re, A. Chiesi-Villa and C. Rizzoli, *Inorg. Chim. Acta*, 1998, **270**, 298–311.
14 D. M. Miller-Shakesby, S. Nigam, D. L. Hughes, E. Lopez-Estelles, M. R. J. Elsegood, C. J. Cawthorne, S. J. Archibald and C. Redshaw, *Dalton Trans.*, 2018, **47**, 8992–8999.
15 (*a*) S. L. Borkowsky, R. F. Jordan and G. D. Hinch, *Organometallics*, 1991, **10**, 1268–1274; (*b*) T. L. Breen and D. W. Stephan, *Inorg. Chem.*, 1992, **31**, 4019–4022; (*c*) J. P. Campbell and W. L. Gladfelter, *Inorg. Chem.*, 1997, **36**, 4094–4098; (*d*) A. Mommertz, R. Leo, W. Massa, K. Harms and K. Dehnicke, *Z. Anorg. Allg. Chem.*, 1998, **624**, 1647–1652; (*e*) B. Birkmann, T. Voss, S. J. Geier, M. Ullrich, G. Kehr, G. Erker and D. W. Stephan, *Organometallics*, 2010, **29**, 5310–5319; (*f*) A. Solovyev, E. Lacôte and D. P. Curran, *Dalton Trans.*, 2013, **42**, 695–700.
16 A. Pärssinen, M. Kohlmayr, M. Leskelä, M. Lahcini and T. Repo, *Polym. Chem.*, 2010, **1**, 834–836.
17 D. Takeuchi, T. Nakamura and T. Aida, *Macromolecules*, 2000, **33**, 725–729.
18 Y. A. Piskun, I. V. Vasilenko, S. V. Kostjuk, K. V. Zaitsev, G. S. Zaitseva and S. S. Karlov, *J. Polym. Sci., Part A: Polym. Chem.*, 2010, **48**, 1230–1240.
19 D. Zhu, L. Guo, W. Zhang, X. Hu, K. Nomura, A. Vignesh, X. Hao, Q. Zhang and W.-H. Sun, *Dalton Trans.*, 2019, **48**, 4157–4167.
20 (*a*) C. Ludwig and M. R. Viant, *Phytochem. Anal.*, 2010, **21**, 22–32; (*b*) M. J. Walton, S. J. Lancaster and C. Redshaw, *ChemCatChem*, 2014, **6**, 1892–1898.
21 (*a*) Z. Zhong, P. J. Dijkstra and J. Feijen, *J. Am. Chem. Soc.*, 2003, **125**, 11291–11298; P. Hormnirun, E. L. Marshall, V. C. Gibson, A. J. P. White and D. J. Williams, *J. Am. Chem. Soc.*, 2004, **126**, 2688–2689.
22 (*a*) Q. Hu, S.-Y. Jie, P. Braunstein and B.-G. Lia, *Chin. J. Polym. Sci.*, 2020, **38**, 240–247; (*b*) M. A. Woodruff and D. W. Hutmacher, *Prog. Polym. Sci.*, 2010, **35**, 1217–1256; (*c*) T. Wu, Z. Wei, Y. Ren, Y. Yu, X. Leng and Y. Li, *Polym. Degrad. Stab.*, 2018, **155**, 173–182; (*d*) M. T. Hunley, N. Sari and K. L. Beers, *ACS Macro Lett.*, 2013, **2**, 375–379.
23 (*a*) F. Della Monica, E. Luciano, A. Buonerba, A. Grassi, S. Milione and C. Capacchione, *RSC Adv.*, 2014, **4**, 51262–51267; (*b*) P. Vanhoorne, P. Dubois, R. Jerome and P. Teyssie, *Macromolecules*, 1992, **25**, 37–44; (*c*) J. Kasperczyk and M. Bero, *Makromol. Chem.*, 1991, **192**, 1777–1787; (*d*) J. Kasperczyk and M. Bero, *Makromol. Chem.*, 1993, **194**, 913–925; (*e*) N. Nomura, A. Akita, R. Ishii and M. Mizuno, *J. Am. Chem. Soc.*, 2010, **132**, 1750–1751; (*f*) G. Li, M. Lamberti, D. Pappalardo and C. Pellecchia, *Macromolecules*, 2012, **45**, 8614–8620.
24 D. Sun, W. Liu, M. Qiu, Y. Zhang and Z. Li, *Chem. Commun.*, 2015, **51**, 2056–2059.
25 (*a*) A. Arduini and A. Casnati in *Macrocycle Synthesis*, ed. D. Parker, Oxford University Press, New York, 1996, ch. 7; (*b*) S. Kim, J. S. Kim, O. J. Shon, S. S. Lee, K.-M. Park, S. O. Kang and J. Ko, *Inorg. Chem.*, 2004, **43**, 2906–2913.
26 Problems with the combustion of calixarene-based complexes have been noted previously, see for example W. Kuran, T. Listos, M. Abramczyk and A. Dawidek, *J. Macromol. Sci., Part A: Pure Appl. Chem.*, 1998, **35**, 427–437.
27 *CrysAlis PRO*, Rigaku Oxford Diffraction, 2017–2018.
28 G. M. Sheldrick, *Acta Crystallogr., Sect. A: Found. Adv.*, 2015, **71**, 3–8.
29 G. M. Sheldrick, *Acta Crystallogr., Sect. C: Struct. Chem.*, 2015, **71**, 3–8.
30 (*a*) A. L. Spek, *Acta Crystallogr., Sect. C: Struct. Chem.*, 2015, **71**, 9–18; (*b*) P. v. d. Sluis and A. L. Spek, *Acta Crystallogr., Sect. A: Found. Crystallogr.*, 1990, **46**, 194–201.